NOAA Technical Memorandum OAR SEC-88

HALLOWEEN SPACE WEATHER STORMS OF 2003

LCDR Michael Weaver, NOAA (editor)
William Murtagh (editor)
Christopher Balch
Doug Biesecker
Larry Combs
Misty Crown
Kent Doggett
Joseph Kunches
Howard Singer
LT David Zezula, NOAA

Space Environment Center
Boulder, Colorado
June 2004

UNITED STATES DEPARTMENT OF COMMERCE
NATIONAL OCEANIC AND ATMOSPHERIC ADMINISTRATION
Office of Oceanic and Atmospheric Research

NOTICE

Mention of a commercial company or product does not constitute an endorsement by NOAA. Use for publicity or advertising purposes of information from this publication concerning proprietary products for the tests of such products is not authorized.

Also available for download at: www.sec.noaa.gov.

CONTENTS

THIS PAGE INTENTIONALLY LEFT BLANK

ABSTRACT

In October and November of 2003, well into the declining phase of Solar Cycle 23, the Sun produced a significant display of solar activity, including one of the most intense solar flares ever recorded. The activity produced by the Sun during this period originated from large and complex sunspot groups. Major solar flare activity was often accompanied by fast Coronal Mass Ejections (CMEs) and strong energetic particle events. The arrival of transient solar wind from Earth-directed CMEs produced extreme geomagnetic storming. Common effects of these space weather phenomena included prolonged high-frequency (HF) communication outages, fluctuations in power transmission systems, and minor to severe impacts on space satellite systems. This technical memorandum outlines the activity observed on the surface of the Sun, the resultant effects in the near-Earth space environment, and the impacts to human-made systems in orbit and on Earth.

1. INTRODUCTION

Solar Cycle 23 began its 11-year cycle in May 1996 with a monthly smoothed sunspot number (SSN) of 8.0, and peaked in April 2000 at 120.8. The early October sunspot count reflected another quiet month in the unremarkable waning phase of an average solar cycle. The quiet period would abruptly end. In stark contrast, and with little warning, large and intense sunspot groups emerged on the solar surface, and by the end of October 2003, NOAA space weather forecasters were engaged in the most active and demanding solar activity epoch in years. In a three week period, staff at the NOAA Space Environment Center (SEC) issued hundreds of space weather watches, warnings, alerts, summaries, and advisories, as the Sun's surface flaunted three of the largest sunspot clusters in over 10 years.

Impacts were wide ranging. Geomagnetically induced currents (GIC) were sufficiently strong over Northern Europe to cause electrical transformer problems and even a power system failure and subsequent blackout. Radiation storm levels were high enough to prompt NASA officials to issue a flight directive to the International Space Station (ISS) astronauts to take precautionary shelter. Airlines took unprecedented actions in their high latitude routes to avoid the high radiation levels and communication blackout areas. Numerous anomalies were reported by deep space missions and by satellites at all orbits. Due to the variety and intensity of this solar activity, most industries vulnerable to space weather experienced some degree of impact to their operations.

The activity received intense coverage by media agencies around the world. SEC staff participated in hundreds of news broadcasts and interviews, assisting media representatives from Chile to Hong Kong. The high levels of activity generated more public and media interest than any other solar event or period this cycle. The heightened public awareness produced enormous interest on the SEC webpage, which saw the daily average hit rate of 500,000 rise to over 19 million hits on 29 October. Solar images and solar activity stories were flashed on newspapers around the world, making "space weather" a household term.

This activity occurred 42 months after Cycle 23's peak in April 2000 (based on solar sunspot number). While late cycle active periods have occurred in the past, it is rare to see this level of activity during this stage of the solar cycle, or even during solar maximum. Seventeen major flares erupted on the Sun between 19 October and 5 November, 2003, including perhaps the most intense flare ever measured on the GOES XRS sensor – a huge X28 flare, resulting in an R5 – extreme radio blackout, on 4 November (see Figure 1 and Table 1). Many of these flares had associated radiation storms, including an S4 (severe) storm on 29 October. There were also several geomagnetic storms, with two of them reaching the G5 (extreme) level on 29 and 30 October. The last occurrence of such late cycle activity was in April and May 1984 during Solar Cycle 21. That period saw a total of nine major flares (between 20 April – 31 May), 52 months after the December 1979 peak of Cycle 21. It should also be noted that 28 major flares occurred in 1973 during the late stages of Cycle 20. Cycle 20 peaked in November 1968.

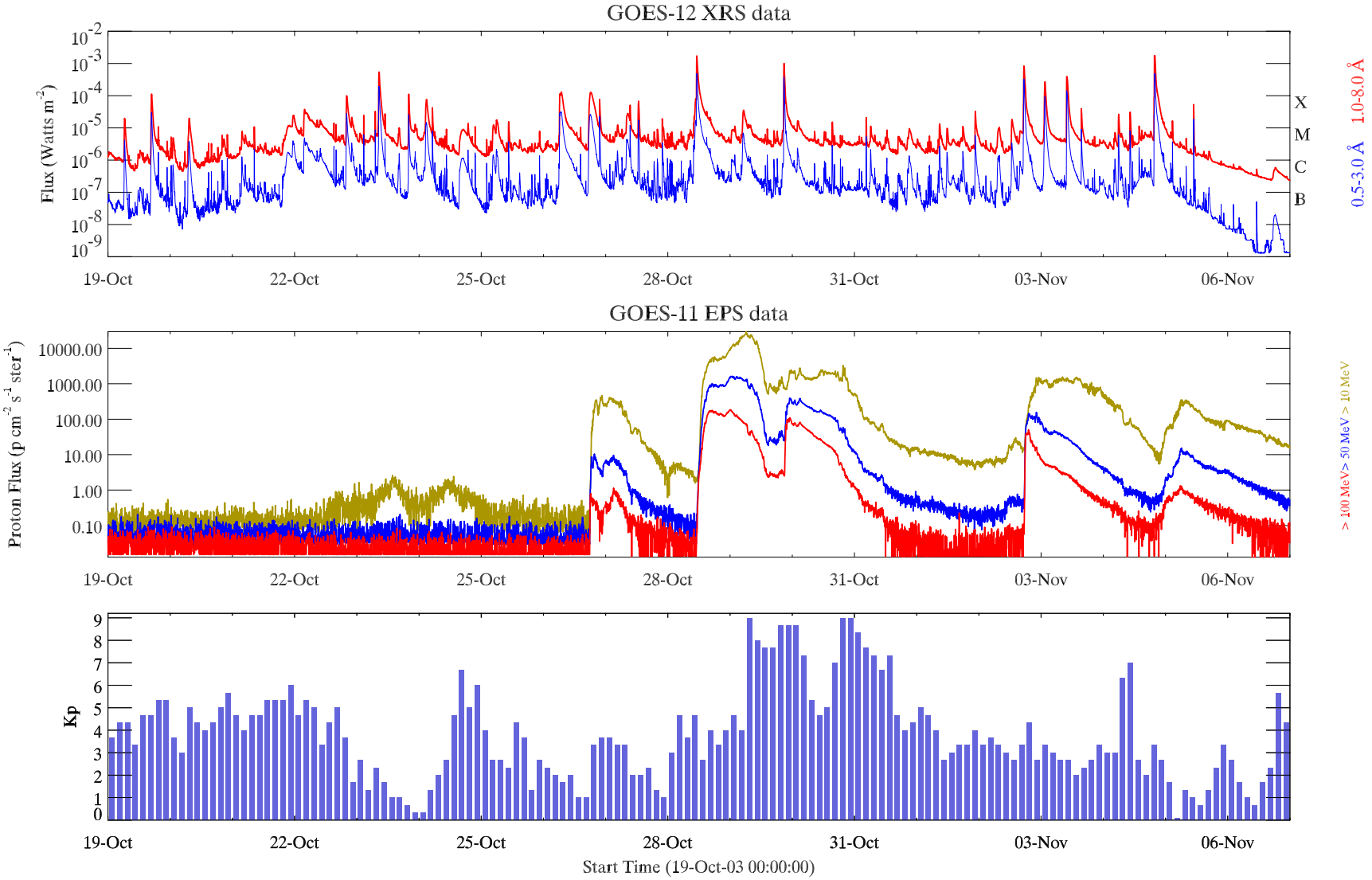

Figure 1: Summary plot of GOES-12 X-ray flux, GOES-11 proton flux, and Planetary Kp index for 23 October to 7 November 2003.

Table 1a: Solar Activity Summary															
X-ray Event and Region						**Radio Emissions**			**Coronal Mass Ejections**				**NOAA Scales**		
Flare Max Date Time	Xray Class	Opt Class	Reg	Location	245 MHz (SFU)	2695 MHz (SFU)	Type II (km/s)	Transit Time (hrs)	Halo Type	Plane of Sky Spd. (km/s)	Shock @ ACE				
19 Oct 1650	X1.1	1n	484	N08E58	650	510	625		P	458		R3		
22 Oct 0351	(Note 1)		484	N07E25		320		59.6	P	651	24/1450	R1		G3
22 Oct 2007	M9.9	Sf	486	S18E78	100	240			P			R2		
23 Oct 0835	X5.4	1b	486	S21E88	10000	1500	967		F	1110		R3		
23 Oct 2004	X1.1	1n	486	S17E84	2500	77						R3		
24 Oct 0254	M7.6	1n	486	S19E72	6800	73						R2		
26 Oct 0654	X1.2	3b	486	S15E44	14000	4000	1302		P	1245		R3		
26 Oct 1819	X1.2	1n	484	N02W38	1100	2000	950	31.8	F	1432	28/0130	R3	S2	G1
26 Oct 2140	M7.6	2n	484	N01W38		57						R2		
27 Oct 0927	M5.0	Sf	486	S16E26		65						R2		
27 Oct 1243	M6.7		486	S17E25	420	59						R2		
28 Oct 1110	X17.2	4b	486	S16E08	490000	13000	1250	19.0	F	2125	29/0559	R4	S4	G5
29 Oct 2049	X10.0	2b	486	S15W02	360000	2500	775	19.0	F	1948	30/1620	R4	S3	G5
02 Nov 1725	X8.3	2b	486	S14W56	24000	7700	1691	37.0	F	1826	04/0600	R3	S3	G3
03 Nov 0130	X2.7	2b	488	N10W83	100	240	1400		P			R3		
03 Nov 0955	X3.9	2f	488	N08W77	3900	4400	869		P			R3		
04 Nov 1950	X28.0	3b	486	S19W83	4800	20000	1268	47.8	F	2381	06/1915	R5	S2	G2
05 Nov 1052	M5.3	Sf	486	S16W90								R2		
Note 2								Note 3, 4			Note 2			

Table 1b: Solar Activity Summary													
X-ray Event		**Geomagnetic Response**				**>10 MeV Proton Event**				**>100 MeV Proton Event**			
Flare Max	**Xray Class**	**SI Time**	**SI Ampl** (nT)	**Max Kp**	**Max Ap**	**Start Time**	**Peak Flux** (PFU)	**Peak Time**	**Dur.** (hr)	**Start Time**	**Peak Flux** (PFU)	**Peak Time**	**Dur.** (hr)
19 Oct 1650	X1.1												
22 Oct 0351	M3.7	24/1529	105	7-	43								
22 Oct 2007	M9.9												
23 Oct 0835	X5.4												
23 Oct 2004	X1.1												
24 Oct 0254	M7.6												
26 Oct 0654	X1.2					26/1825	466	26/2235	24.8				
26 Oct 1819	X1.2	28/0207	10										
26 Oct 2140	M7.6												
27 Oct 0927	M5.0												
27 Oct 1243	M6.7												
28 Oct 1110	X17.5	29/0613	140	9_0	252	28/1215	29525	29/0615	94.7	28/1150	186	29/0015	61.9
29 Oct 2049	X10.0			9_0	221	29/2150	3298	29/1935	61.1	29/2150	110	29/2310	27.9
02 Nov 1725	X8.3	04/0627	72	7_0	39	02/1745	1570	03/1345	51.6	02/1740	49	02/1905	23.7
03 Nov 0130	X2.7												
03 Nov 0955	X3.9												
04 Nov 1950	X28.0	06/1937	31	6-	20	04/2225	353	05/0600	62.1	05/0535	1.3	05/0540	1.5
05 Nov 1052	M5.3												
Note 2		Note 5		Note 2, 6		Note 2, 7		Note 2, 8		Note 2			

Notes:

1. This was a complex event with two distinct filament eruptions north and south of Region 484. An M3.7/Sf x-ray flare occurred at the same time in Region 486. The resulting geophysical activity was likely due to the DSFs.
2. All dates and times are in universal time (UTC).
3. From maximum of X-ray event to the time of sudden impulse.
4. The transit time for the CME associated with the X10 flare on 29 October is estimated since there was no sudden impulse from the shock arrival.
5. Sudden impulse measured at the Boulder magnetometer.
6. Kp and Ap values are from Postdam.
7. Start time of 29/2150 for the >10 MeV proton event is the time of onset of secondary enhancement. The >10 MeV proton event from 28/1215 was still in progress. The >10 MeV proton event end time for both events are the same – the time proton levels dropped below the 10 PFU threshold.
8. Start time of 29/2150 for the >100 MeV proton event is the time of secondary enhancement onset. The >100 MeV proton event from 28/1150 was still in progress. The >100 MeV proton event end time for both events are the same – the time proton levels dropped below the 1 PFU threshold.

2. SOLAR ACTIVITY

Solar activity from 19 October to 5 November 2003 originated from three large and complex sunspot regions. SEC Space Weather Operations numbered these sunspot clusters as Region 484, Region 486, and Region 488. While each of these regions was remarkable in size and magnetic complexity, Region 486 was by far the most significant, with a maximum area of 2610 millionths.[1] It became the largest sunspot group of Solar Cycle 23 and the largest region since 1991. Of the 17 major flares that occurred during this period 12 were from Region 486, including an X17 on 28 October, an X10 on 29 October, and an X28 (estimated) on 4 November.

a. Analysis of Major Solar Active Regions

Region 484 (Figure 2) rotated onto the visible disk on 18 October at 200 millionths in size in a beta magnetic configuration.[2] Its existence was suspected a few days before it could be seen on the east limb. Increased X-ray background levels were observed on 17 October and increased EUV flux emissions noted in EIT imagery. Region 484 grew rapidly on 19 October to just over 1000 millionths and significantly increased in magnetic complexity. This remarkable emergence of new flux included the formation of a strong delta configuration across a complex northeast-to-southwest polarity inversion line. From 20 to 22 October, this region continued to increase in size and magnetic complexity reaching an area of 1750 millionths with multiple delta magnetic configurations within one large penumbral area. As Region 484 transited the central meridian it began to slowly decay, decreasing to 1250 millionths by 29 October. The region rotated around the west limb on 31 October. Throughout this gradual decay in sunspot area coverage the magnetic complexity did not appear to diminish. Multiple delta configurations were evident until the region transited the west limb. Figure 5 illustrates the development of Region 484 as it rotated across the visible disk.

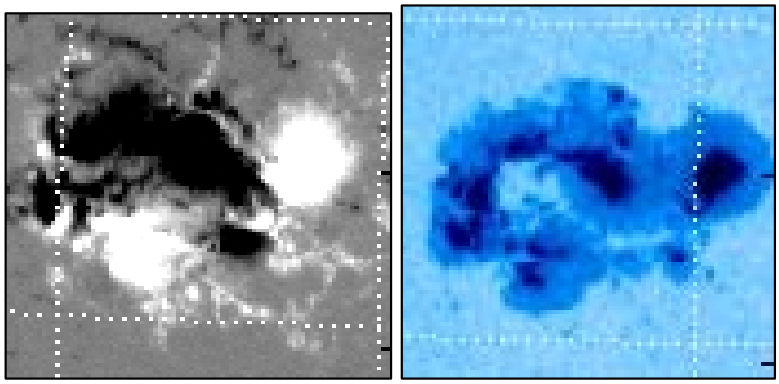

Figure 2: Region 484 magnetic configuration (left) and white light (right) on 22 October 2003. (Images courtesy of NASA and Big Bear Solar Observatory, BBSO)

Powerful CMEs were observed from a source behind the southeast limb on 19 to 21 October, suggesting another volatile sunspot cluster would soon appear. Region 486 (Figure 3) rotated onto the visible disk on 22 October and was in full view by 23 October. Unlike Region 484, which grew rapidly after appearing on the disk, Region 486 was large and complex from its first appearance. Multiple magnetic delta configurations were obvious and a sunspot area exceeding

[1] A description of acronyms and terms used in this memorandum can be found in Appendix A.
[2] For more details about how SEC describes the visible and magnetic configurations of solar active regions, see SEC's education website at **http://sec.noaa.gov/education**.

1100 millionths was observed as soon as the region was fully visible. Though already large and complex, Region 486 was still in a growth phase and continued to develop over the next six days, reaching its largest size of 2610 millionths by 29 October and becoming the largest sunspot cluster of Solar Cycle 23. On 27 October, Region 486 developed an east-west corridor of negative polarity through positive polarity. Significant magnetic shear evolved along an extended complex inversion line. As a result, two of the larger X-ray events, an X17 and X10 on 28 and 29 October, respectively, occurred just after this east-west inversion line formed. Region 486 began a slow decay on 30 October. However, a tremendously complex magnetic configuration persisted through the remainder of the region's visible disk transit. Region 486 rotated around the west limb on 5 November, but continued to produce powerful CMEs for several days after its exit from the visible disk. Figure 6 illustrates the development of Region 486 as it rotated across the visible disk.

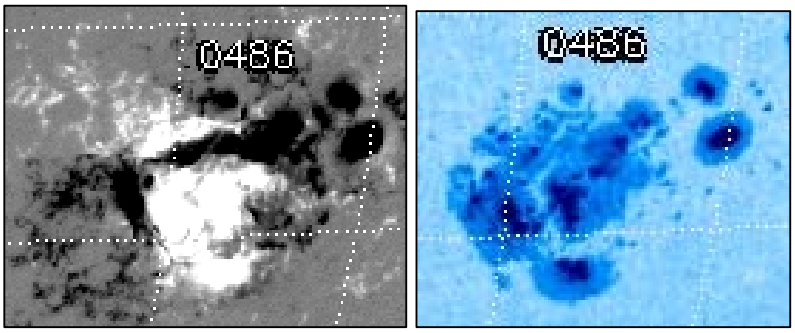

Figure 3: Region 486 magnetic configuration (left) and white light (right) on 30 October 2003. (Images courtesy of NASA & BBSO)

Region 488 (Figure 4) formed on the visible disk near N09E22. The spots emerged on 26 October and grew very rapidly over the next three days. By 28 October, Region 488 was at 800 millionths and by 29 October at 1460 millionths. With the rapid growth phase the region also developed significant magnetic complexity. A beta-gamma-delta magnetic configuration formed on 28 October and persisted for the remainder of the disk passage. Region 488 reached maximum area coverage of 1750 millionths on 30 October. A slow decay began on 31 October and continued until the region transited the west limb on 4 November. The large extent between the leader and trailing spots resulted in limited compactness of intermediate spots. This may explain the limited X-ray production by this region: only two major flares originated from Region 488. Figure 7 illustrates the development of Region 488 as it rotated across the visible disk.[3] Figure 8 illustrates all three major solar active regions in a hydrogen-alpha synoptic image.

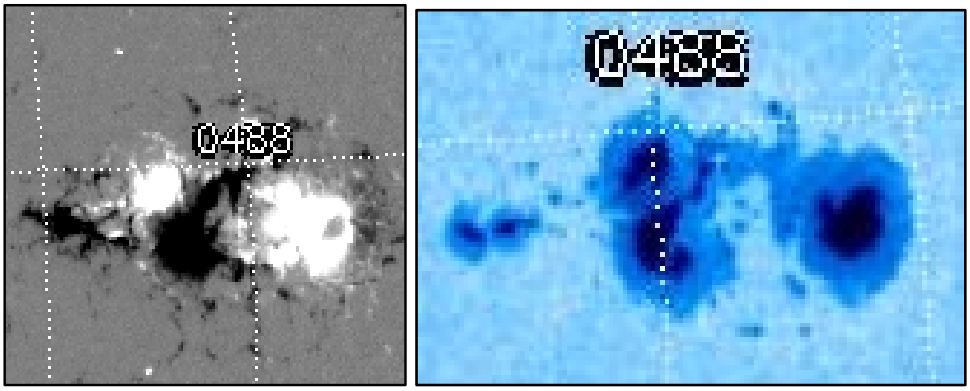

Figure 4: Region 488 magnetic configuration (left) and white light (right) on 30 October. (Images courtesy of NASA & BBSO)

[3] Imagery for Figures 2 through 7 was compiled courtesy of data from the Active Region Monitor (ARM) of NASA's Goddard Space Flight Center and Big Bear Solar Observatory. See **http://beauty.nascom.nasa.gov/arm** for more information.

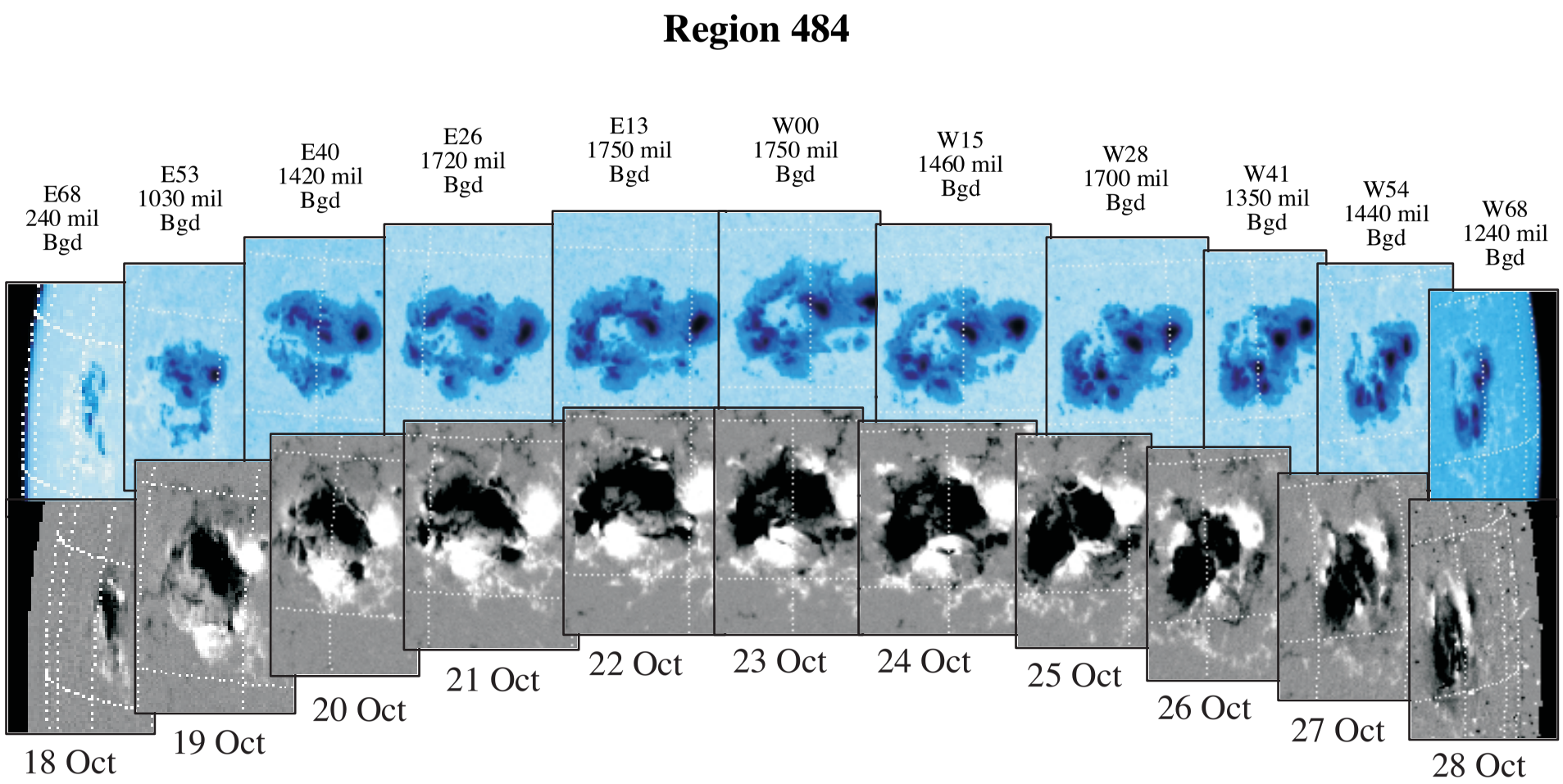

Figure 5: Development of Region 484 (Images courtesy of Big Bear Solar Observatory)

Region 486

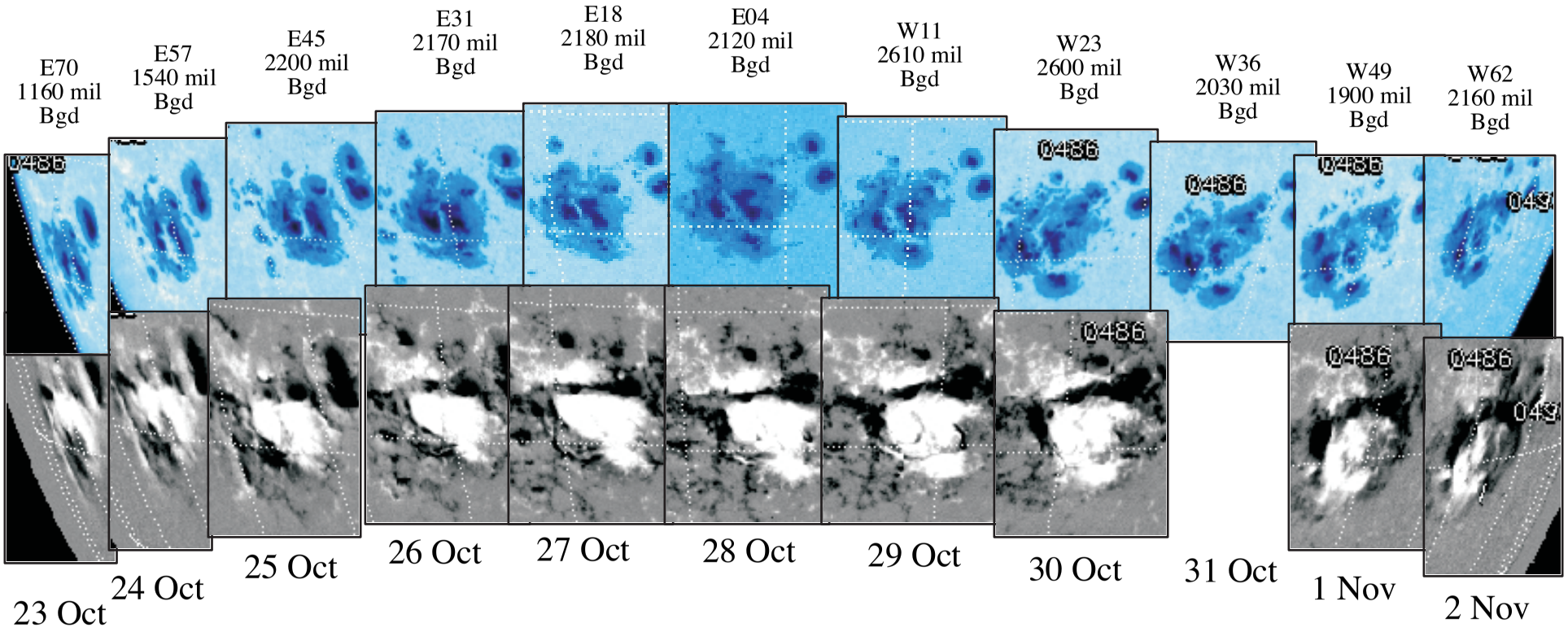

Figure 6: Development of Region 486 (Images courtesy of Big Bear Solar Observatory)

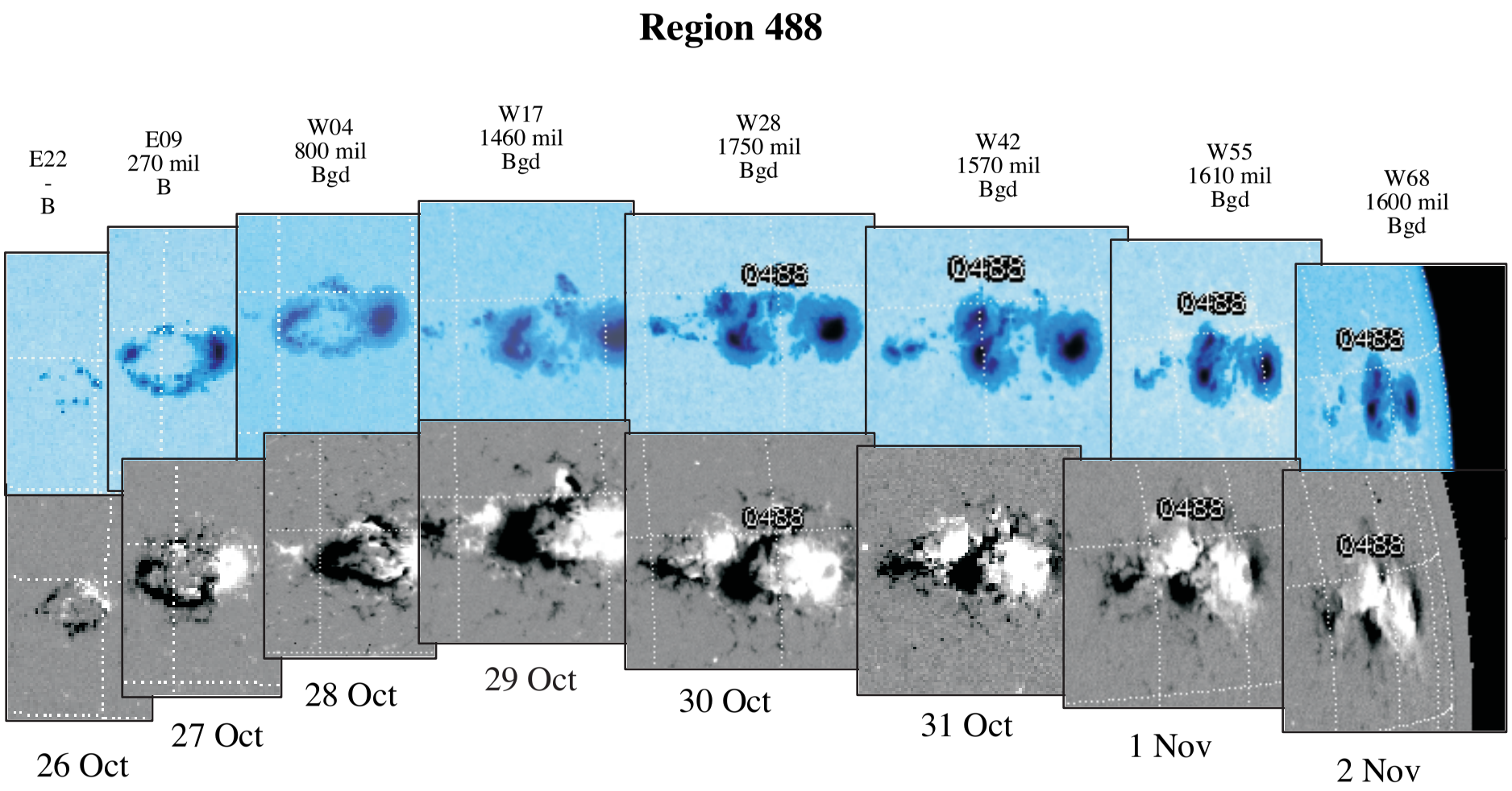

Figure 7: Development of Region 488 (Images courtesy of Big Bear Solar Observatory)

Hydrogen-Alpha Synoptic "Image"

Oct - Nov 2003

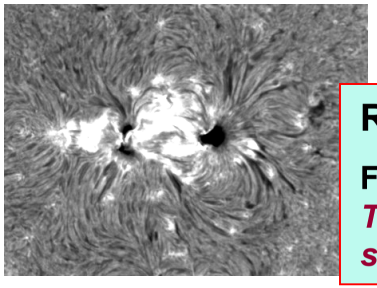

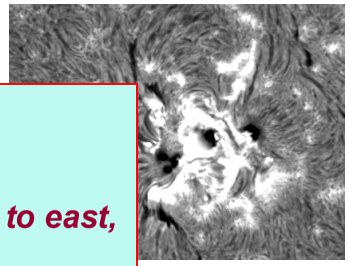

Region 488

Flares: 7M, 2X;
Transequatorial surging

Region 484

Flares: 16M, 2X
Repeated surging to east, and a bright wave

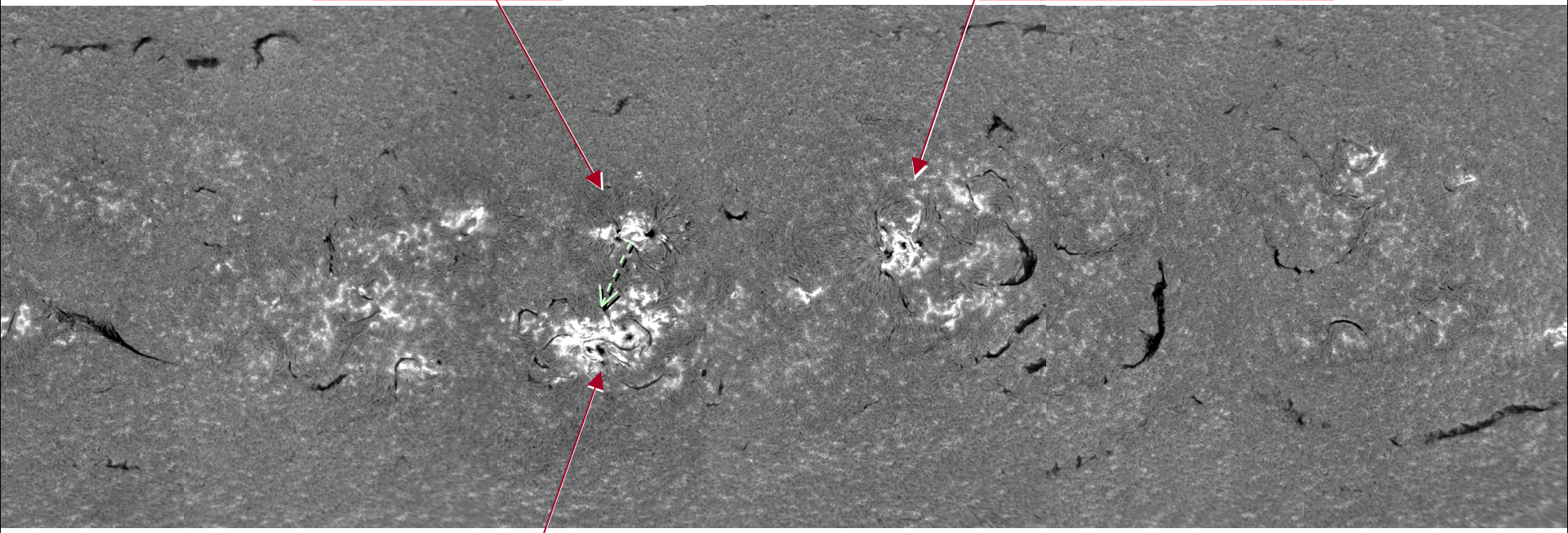

180 240 300 360 60 120

Carrington

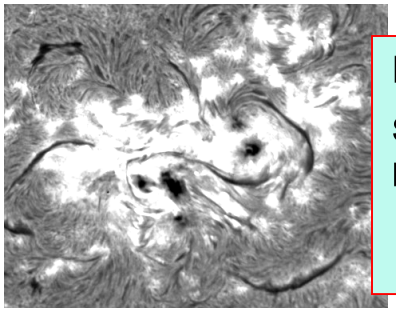

Region 486 **Flares: 18M, 4X, 2X^{+}**

Several spectacular flare waves & propagating disturbances: 29 Oct and 4 Nov

Flare waves follow a similar directional pattern on both 29 Oct and 4 Nov

Figure 8: Hydrogen-Alpha Synoptic Image (courtesy of U.S. Air Force ISOON)

b. X-Ray Flares, Radio Emissions, and Solar Imagery

Major solar activity began on 19 October as Region 484 rotated around the east limb. An X1 (1n) flare occurred at 1650 UTC near N08E58. Associated with this flare was a Type II radio sweep 630 km/s[4] and a 510 SFU tenflare. LASCO imagery revealed a partial halo Coronal Mass Ejection (CME) with a plane-of-sky speed measured at 460 km/s. As Region 486 rotated onto the disk it produced an M9 (Sf) at 2007 UTC on 22 October, near S18E78. A complex filament eruption near Region 484 occurred early on 22 October and produced an Earth-directed CME. This CME was the mostly likely source of the shock and transient flow observed on 24 October, which produced a brief period of severe geomagnetic storming.

Table 2: Top Flares Since 1976

Rank	*Date*	*X-ray*	*Region*
1	**11/04/03**	**X28e**	**486**
2	08/16/89	X20e	5629
3	04/02/01	X20e	9393
4	**10/28/03**	**X17**	**486**
5	07/11/78	X15e	1203
6	03/06/89	X15e	5395
7	04/24/84	X13e	4474
8	10/19/89	X13e	5747
9	06/06/82	X12e	3763
10	06/01/91	X12e	6659
11	12/15/82	X12	4026
12	06/04/91	X12e	6659
13	06/06/91	X12e	6659
14	06/11/91	X12e	6659
15	06/15/91	X12e	6659
16	12/17/82	X10	4025
17	05/20/84	X10	4492
18	01/25/91	X10	6471
19	06/09/91	X10	6659
20	**10/29/03**	**X10**	**486**

NOTE: Flares with an "e" suffix are estimated due to saturation of the GOES XRS instrument. The saturation level was increased to X17 in 1993.

Region 486 continued to produce major flares on 22-24 October with two X-class flares and an M-class flare. An X5 (1b) flare occurred at 0835 UTC on 23 October near S21E88. Significant radio emissions were associated with the event including a Type II radio sweep (970 km/s), a 1500 SFU tenflare, and a 10,000 SFU 245 MHz radio burst. EIT and LASCO imagery revealed a large EIT wave with dimming and a full halo CME associated with this flare, although the CME was not Earth-directed. The second X-class event on 23 October was an impulsive X1 (1n) at 2004 UTC near S17E84. Radio emissions observed from this flare included a 2,500 SFU radio burst at 245 MHz. Early on 24 October, Region 486 produced an M7 (1n) at 0254 UTC near S19E72. A Type IV radio sweep and 245 MHz radio burst (6,800 SFU) were associated with this flare. LASCO imagery observed a CME with a plane-of-sky speed of 900 km/s that was directed to the east and not towards Earth.

On 26 October, Regions 484 and 486 each produced major flare activity. Region 486 produced an X1 (3b) at 0654 UTC near S15E44. This flare was associated with powerful radio emissions including Type II (1,300 km/s) and Type IV radio sweeps, a 120,000 SFU burst on 245 MHz and a 4,400 SFU tenflare. Though this tenflare was modest in comparison to tenflares observed later in this period, other centimetric wavelength measurements were some of the highest ever recorded. These included a remarkable 530,000 SFU burst on 410 MHz and 516,000 SFU on 610 MHz. The radiotelescope saturated for short periods on both frequencies, so peak flux was likely higher than those reported (see Figure 13).

[4] Radio sweep speeds and CME plane-of sky speeds are accurate to two significant digits unless otherwise specified.

LASCO imagery indicated an associated partial halo CME with a plane of sky speed measured at 1,200 km/s. A large EIT wave and dimming were observed in EIT imagery. Later in the day, Region 484 produced an X1 (1n) at 1819 UTC near N02W38. Radio emissions associated with this event included a Type II (950 km/s) radio sweep, 1,100 SFU 245 MHz radio burst and a 2,000 SFU tenflare. A large EIT wave with dimming was observed in EIT imagery and a full halo CME, with a plane-of-sky speed of 1,400 km/s, was observed in LASCO imagery. This flare was also the likely source of an energetic particle event that began later in the day and a shock that was observed at ACE on 28 October at 0130 UTC. As X-ray levels were declining from the second X1 flare, an impulsive M7 (2n) flare erupted at 2140 UTC from Region 484. No significant radio emissions or CME were associated with this flare.

On 27 October, Region 486 produced two major M-class events. The first was an impulsive M5 at 0927 UTC near S16E26 with only minor radio emissions. The second was an M6 at 1243 UTC near S17E25 and was associated with a minor 245 MHz radio burst of 420 SFU.

The most significant solar activity of the late October–early November period began on 28 October. At 1110 UTC, an X17 (4b) flare occurred from Region 486, near S16E08. This was the only 4b flare observed during Solar Cycle 23. Type II (1,300 km/s) and Type IV radio sweeps were observed as well as a 13,000 SFU tenflare and an intense 490,000 SFU 245 MHz radio burst. The 245 MHz burst reached the instrumentation limit and was probably higher. EIT imagery indicated a large EIT wave with significant dimming. LASCO imagery revealed a very fast, full halo CME with a plane of sky speed measured at 2,100 km/s (see Figure 9). The event was promptly followed by an energetic >10 MeV proton event that exceeded the 1,000 PFU level within an hour and the 10,000 PFU level within 13 hours. The CME-driven shock arrived at Earth on 29 October at 0613 UTC in just 19 hours. This was the fastest Sun – Earth transit of a CME this cycle. The geomagnetic storm that followed reached extreme (G5) levels and lasted for 27 hours.

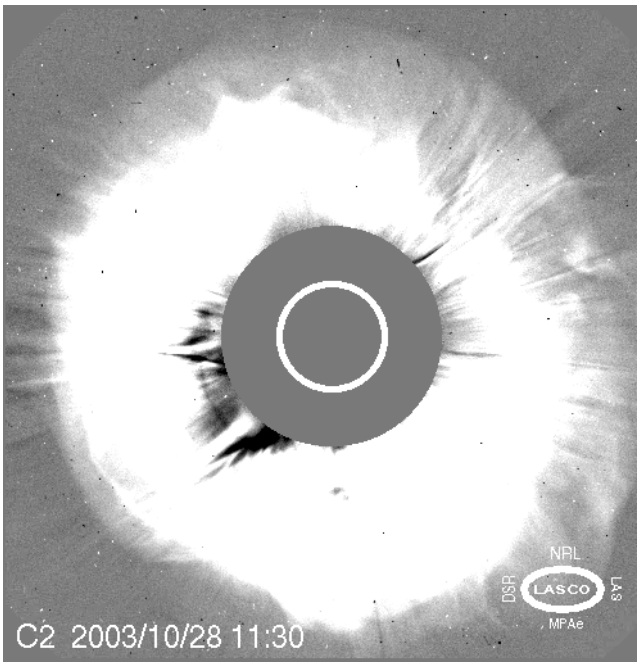

Figure 9: Full halo CME from X17.4 flare on LASCO imagery, 28 October 2003. (Image courtesy of NASA)

Region 486 produced another significant major flare on 29 October. An X10 (2b) flare erupted at 2049 UTC from near S15W02. This flare was also associated with strong radio emissions that included Type II (780 km/s) and Type IV radio sweeps, a 360,000 SFU 245 MHz radio burst and a 2,500 SFU tenflare. EIT imagery revealed a large wave and significant dimming. LASCO imagery showed a very fast full halo CME associated with this flare. The plane of sky speed was measured at 1,900 km/s, representing another extremely fast CME. The transit time for this

CME was 19 hours, arriving at Earth at 1600 UTC on 30 October. The geomagnetic storm from this CME lasted for 24 hours and reached extreme levels. At the time of this flare, a proton event was still in progress due the X17 flare on the 28 October, but the proton flux was on the decline when the X10 flare occurred. The X10 flare produced a secondary enhancement of energetic protons.

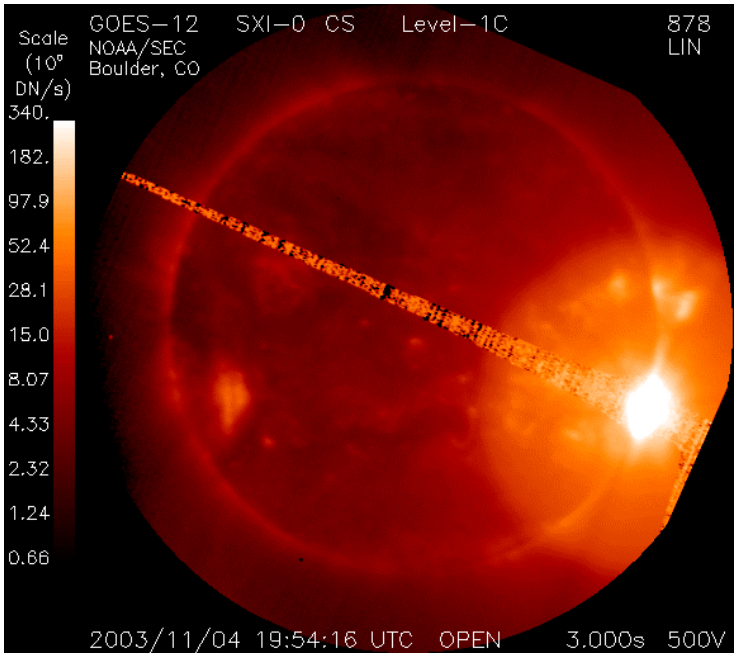

Figure 10: GOES SXI Imagery of the X28 (estimated) flare on 4 November 2003.

Activity was relatively quiet until 2 November when Region 486 produced yet another major flare. An X8 (2b) occurred at 1725 UTC near S14W56. Strong radio emissions were associated with this event, including Type II (1,700 km/s) and Type IV radio sweeps, a 24,000 SFU 245 MHz radio burst and a 7,700 SFU tenflare. A very large wave and dimming was visible in EIT imagery. LASCO imagery indicated a full halo CME, with a plane of sky speed measured at 1,800 km/s. The geomagnetic response was observed at Earth around 0630 UTC on 4 November as a brief geomagnetic storm.

Region 488 produced two major flares near the end of its disk passage on 3 November. The first flare was an X2 (2b) at 0130 UTC near N10W83. Radio emissions included Type II (1,400 km/s) and Type IV radio sweeps as well as a minor 245 MHz radio burst and tenflare. LASCO imagery showed a partial halo CME associated with the X2 flare. The second major flare from Region 488 was an X3 (2f) at 0955 UTC near N08W77. A Type II (870 km/s) and Type IV radio sweep were associated with the X3 flare as well as a 3,900 SFU 245 MHz radio burst and a 4,400 SFU tenflare. LASCO imagery indicated a partial halo CME off the northwest limb.

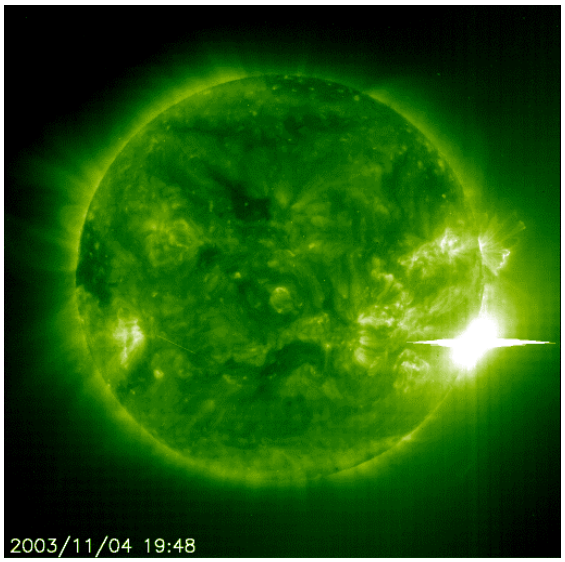

Figure 11: SOHO/EIT Imagery of the X28 (estimated) flare on 4 November 2003. (Image courtesy of NASA)

One of the most powerful solar events during the October-November period was the X28 (estimated) major flare from Region 486 (Figures 9 and 10). The X28 (3b) flare occurred on 4 November at 1950 UTC near S19W83. The GOES XRS instrument was saturated at the X17 level for 12 minutes during this flare. Using historical flare data and mathematical

modeling the peak flux was estimated to be X28. This flare is likely the most intense flare observed since 1976 when GOES X-ray measurement of solar flares began, although there are other flares in the record that also saturated the sensor. Radio emission from this flare included Type II (1,300 km/s) and Type IV radio sweeps and a 4,800 SFU radio burst at 245 MHz and a 20,000 SFU tenflare. EIT 195 imagery showed a very large wave and significant dimming. LASCO imagery indicated an associated full halo CME, measuring a plane of sky speed of 2,400 km/s (Figure 12). Despite the record size of the flare and high speed of the CME, its location near the west limb of the Sun limited its impact at Earth. The center of the CME was directed off the southwest limb and was observed as a glancing blow at Earth. Minor storm conditions were observed for a brief 3-hour period on 6 November. A moderate proton event associated with this flare lasted for about 3 days and ended late on 7 November.[5]

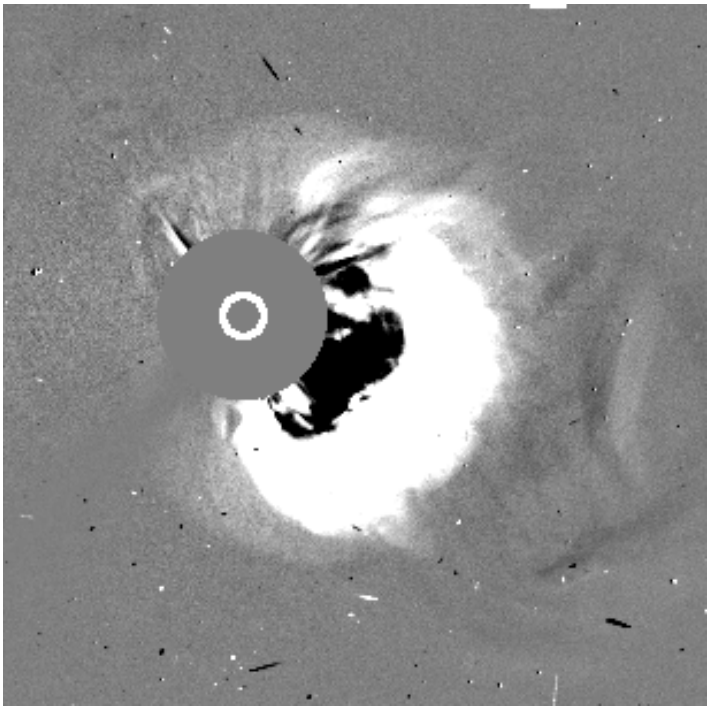

Figure 12: Full halo CME from X28 (estimated) flare on LASCO imagery on 4 November 2003. (Image courtesy of NASA)

The last major flare of the period was an impulsive M5 (Sf) that occurred at 1052 UTC on 5 November. This flare was located on the southwest limb and Region 486 was the most likely source. No significant radio emissions or CMEs were associated with this event.

Powerful eruptions continued for over a week after Region 486 and 488 rotated around the west limb. Several large and fast back-sided full halo CMEs were observed on LASCO imagery from 5 through 12 November. Region 484 rotated back into view on the east limb on 13 November and was responsible for a powerful geomagnetic storm on 20 November (Dst: -472). Full sky Lyman-alpha measurements from the Solar Wind Anisotropies (SWAN) team indicated that activity levels decreased considerably from Regions 486 and 488 on 15 November. Both regions rotated back onto the visible disk on 18 and 19 November with moderate size and complexity. On their second transit of the visible disk, they produced only C-class and isolated M-class flares, and old Region 486 was responsible for a small proton event on 2 December.

[5] SXI Imagery was unavailable until 28 October 2003 because the instrument experienced a high voltage anamoly on 2 September 2003. NOAA's Satellite Operations Control Center was still diagnosing the problems with SXI as increased levels of solar activity began in late October. SEC requested that the SXI operations be resumed, and real-time SXI imagery was made available to SEC on 28 October 2003.

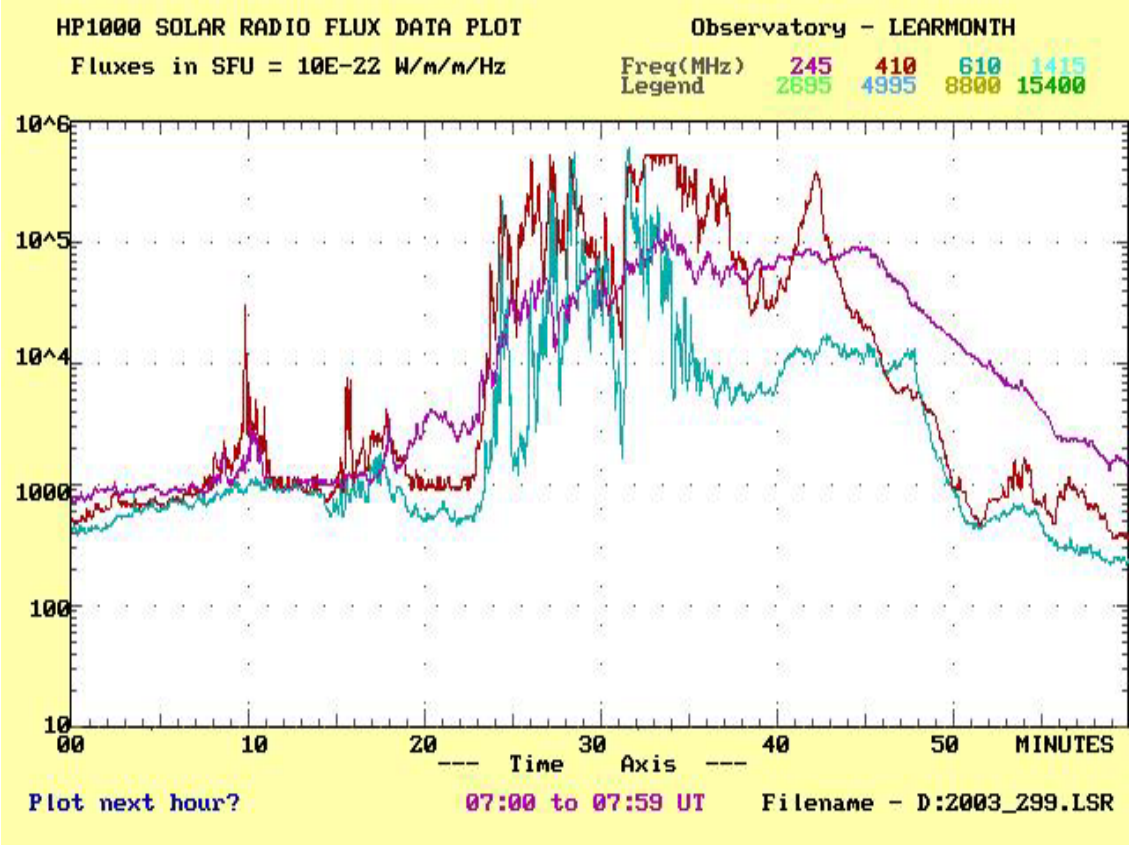

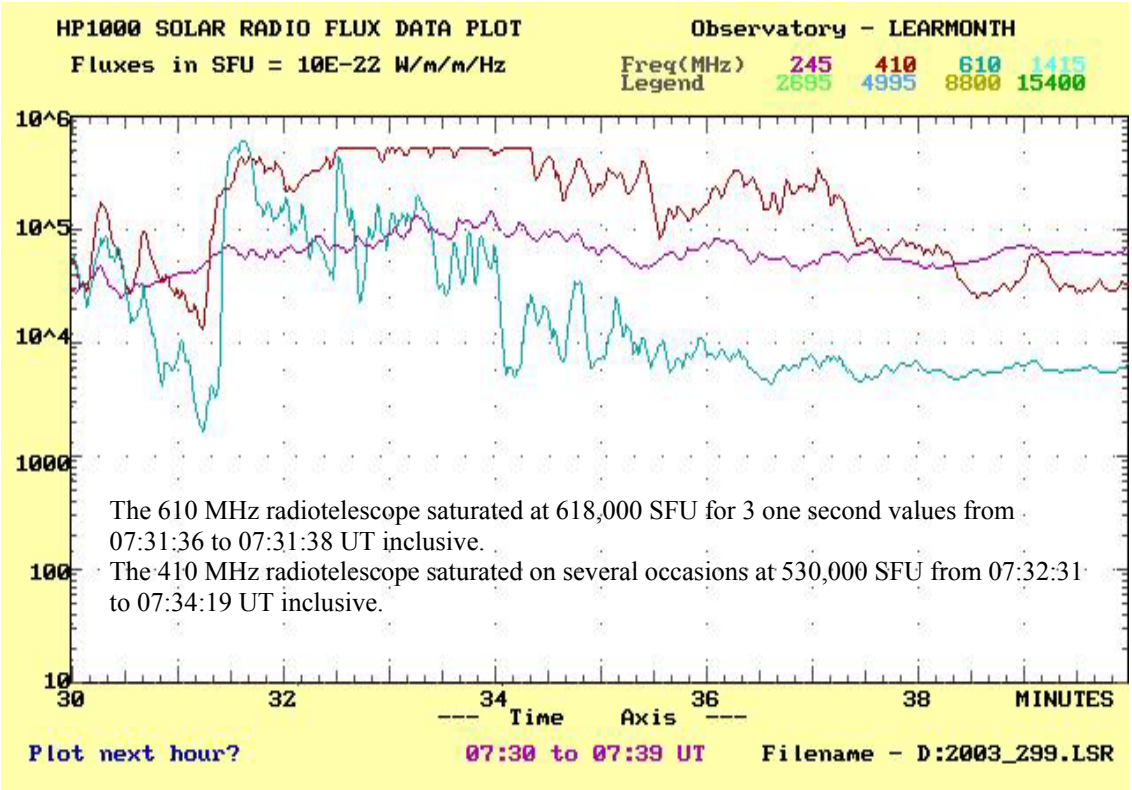

Figure 13. The powerful 26 October radio burst (Courtesy of John Kennewell, IPS Australia).

3. SOLAR WIND: ACE MEASUREMENTS

The NASA Advanced Composition Explorer (ACE) spacecraft is an important asset for SEC to support real-time space weather operations. Although ACE is primarily a research spacecraft, it was modified to add the capability to continuously transmit a subset of its solar wind and energetic particle data from its station between the Sun and Earth, approximately 1.5×10^6 km from Earth. The NOAA Real-Time Solar Wind (RTSW) System gathers solar wind and energetic particle data from four instruments: Magnetic Fields (MAG); Solar Isotope Spectrometer (SIS); Solar Wind Electron Proton Alpha Monitor (SWEPAM); and the Electron, Proton, and Alpha Monitor (EPAM). These data provide valuable information to space weather forecasters on the physical characteristics of the solar wind, the embedded Interplanetary Magnetic Field (IMF), and energetic electron and proton particle fluxes within a variety of energy ranges (Zwickl, et. al., 1998).

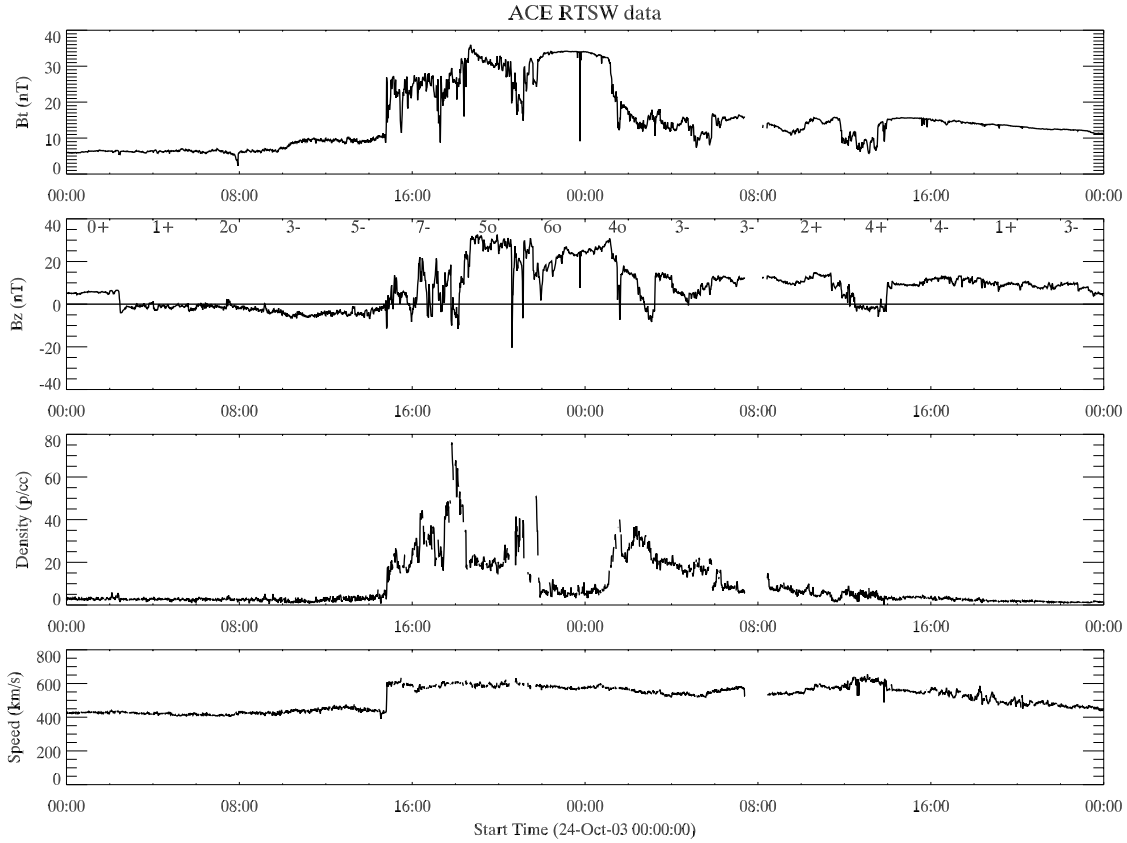

Figure 14: ACE RSTW and Magnetic Field Data for 24-25 October 2003

a. ACE Shock and Transient Flow Observations

24 October, 1450 UTC

ACE observed a shock on 24 October at 1450 UTC. This shock was driven by a full-halo CME that erupted from the solar surface early on 22 October. The arrival of the shock was indicated by a rapid rise of solar wind speed from 400 to 600 km/s, and a significant increase of the

interplanetary magnetic field strength (B_T) up to 30 nT (see Figure 14). Several hours prior to shock arrival, ACE EPAM particle data started to increase, indicating the likely arrival of an approaching CME shock. Subsequent to the shock, the interplanetary magnetic field was primarily northward (Bz>0) with the exception of some brief periods of southward Bz immediately following the shock arrival. The sudden impulse at Earth was observed 40 minutes after the shock passage at ACE (at 1530 UTC), and the ensuing severe geomagnetic storm lasted for 2 hours, with a maximum Kp=7-.

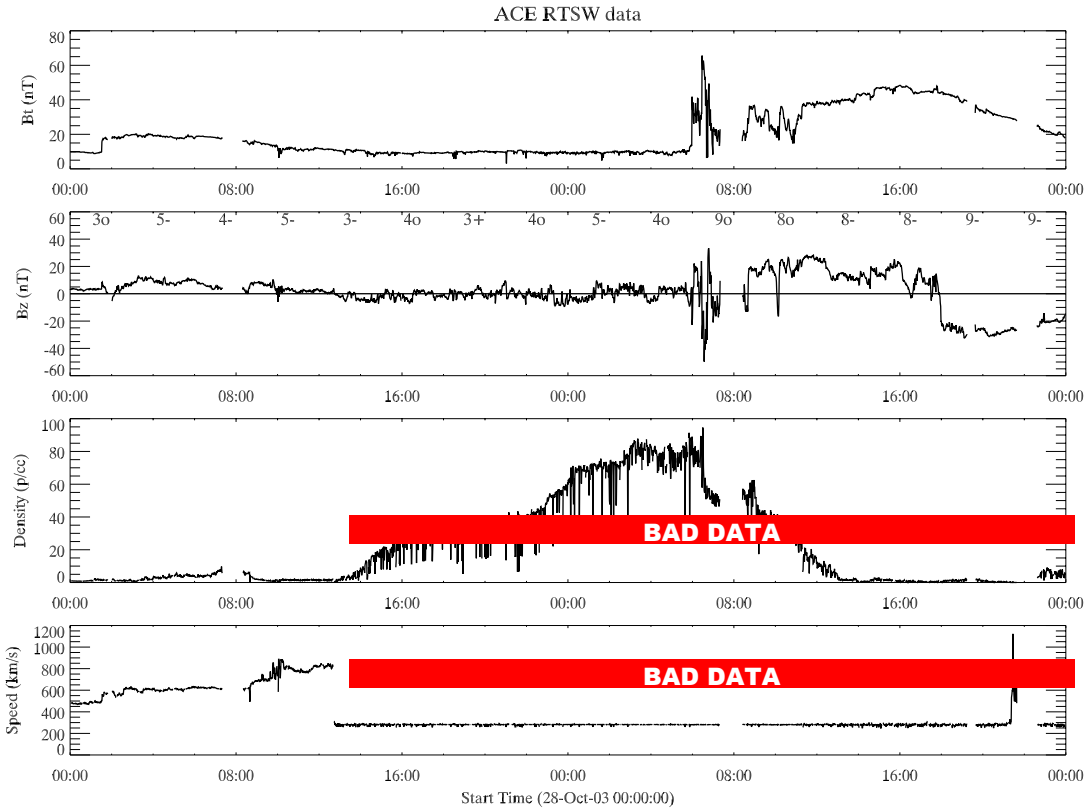

Figure 15: ACE RSTW and Magnetic Field Data for 28-29 October 2003 (speed and density data are invalid after 1200 UTC on 24 October due to contamination from high fluxes of high energy particles)

28 October, 0130 UTC

A full-halo CME erupted from the Sun associated with an X1 flare observed on 26 October at 1819 UTC. The shock driven by this fast CME arrived at 0130 UTC on 28 October (see Figure 15). Solar wind speed increased from 450 to 570 km/s, and the total magnetic field increased from 10 to 20 nT. Again, Bz maintained a generally northward orientation, with the exception of a very brief interval of southward orientation shortly after the shock arrived. As a result, the geomagnetic disturbance on Earth was limited to isolated periods of minor storming (Kp=5-).

29 October, 0559 UTC

At 1100 UTC on 28 October, an X17 flare erupted on the Sun, with an associated full-halo CME. The ACE EPAM particle flux increased steadily several hours before the shock arrival with a

notably sharp increase at the time of the shock. The shock from this CME was observed at ACE at 0559 UTC on 29 October (see Figure 15). A sudden impulse at Earth was observed at 0613 UTC, and was followed by periods of extreme geomagnetic activity ($Kp=9_0$). The total interplanetary magnetic field increased dramatically at the time of shock arrival, with the southward Bz peaking at –50 nT. By 1800 UTC, after an extended interval of northward orientation, Bz rotated southward to near –30 nT for a period of several hours. ACE solar wind plasma measurements from the ACE/SWEPAM were unavailable from 1220 UTC on 28 October until 0100 UTC on 31 October, due to contamination from high fluxes of energetic particles from the proton event associated with the X17 flare. During the outage, a different non-real-time data mode on the SWEPAM sensor was used to approximate the maximum solar wind speed at approximately 2,000 km/s (see Section 3.b. below).

30 October, 1620 UTC

ACE observed a shock driven by a full-halo CME associated with an X10 flare that erupted from the Sun on 29 October at 2049 UTC. The shock was observed on 30 October at 1620 UTC as indicated by the sharp rise in B_T, and was followed by a long period of strongly southward Bz reaching –30 nT (see Figure 16). The ensuing geomagnetic storm lasted for 24 hours with a maximum $Kp=9_0$ at Boulder. ACE RTSW/SWEPAM measurements remained unavailable during this event.

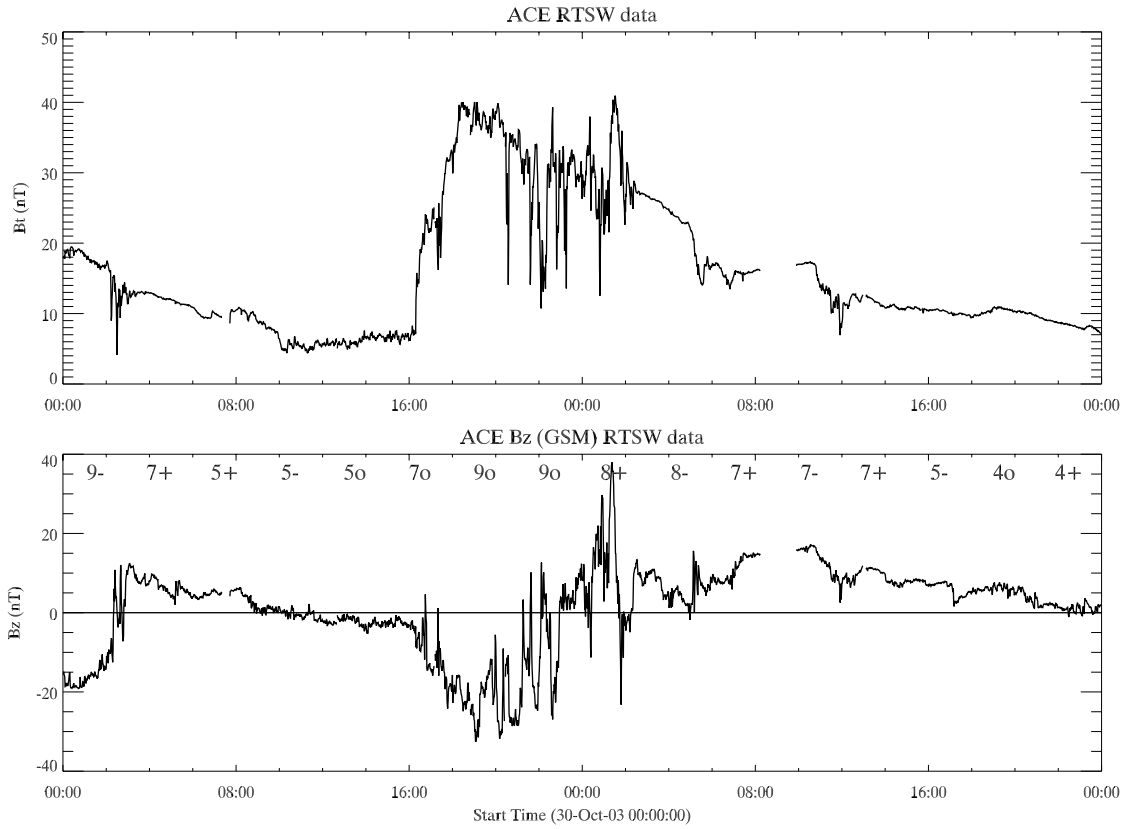

Figure 16: ACE RSTW Magnetic Field Data for 30-31 October 2003

4 November, 0600 UTC

A full-halo CME erupted from the Sun associated with an X8 flare on 2 November at 1725 UTC. The shock arrived at 0600 UTC on 4 November (see Figure 17). Solar wind speed increased from 500 to 775 km/s, and the total magnetic field increased from 7 to 25 nT. Following the shock, Bz maintained a mostly northward orientation (up to 20 nT) for the first few hours, and then turned southward. The southward turning of the magnetic field resulted in major geomagnetic storming (Kp=7_0).

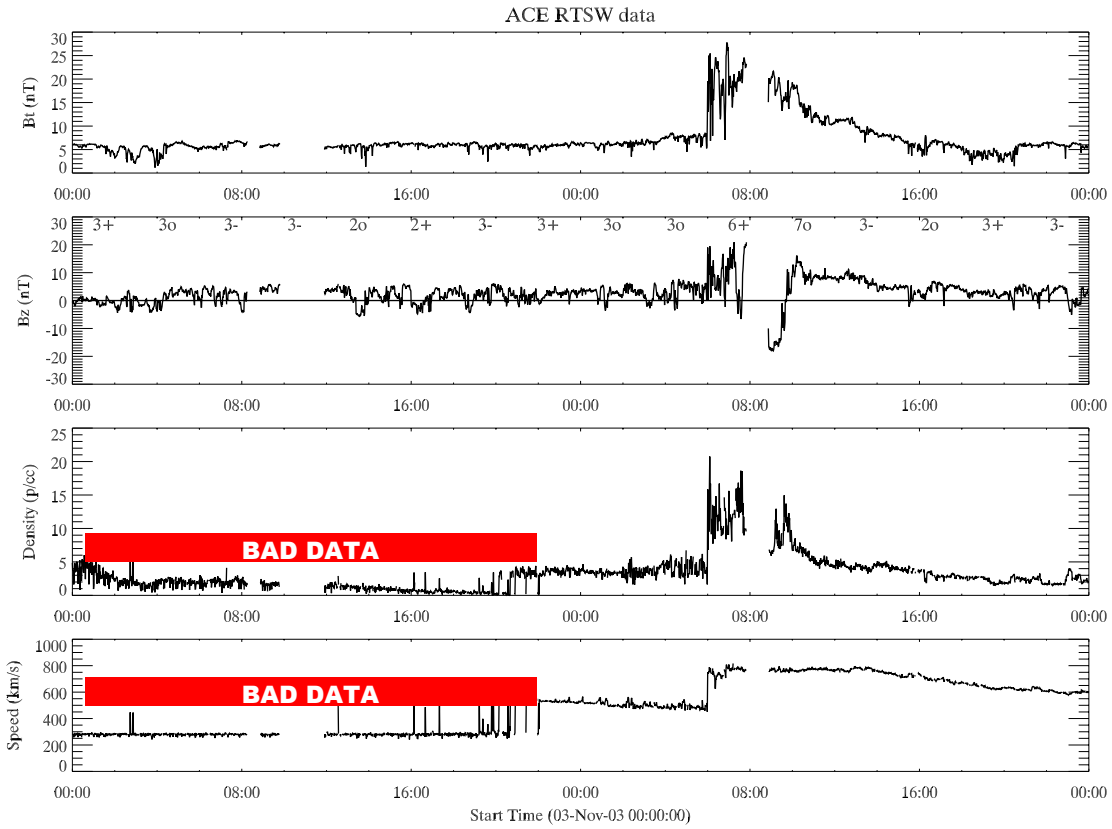

Figure 17: ACE RSTW Data for 3-4 November 2003 (speed and density data are invalid until 2200 UTC on 4 November due to contamination from high fluxes of high energy particles)

6 November, 1937 UTC

A CME associated with the X28 flare that erupted on the west limb on 4 November resulted in a small shock observed at ACE on 6 November at 1937 UTC. Though a full halo CME was identified on LASCO, the center of the CME was not Earth-directed, and the solar wind measurements from ACE were consistent with a glancing blow. Solar wind velocity jumped from 500 to 600 km/s, particle density increased, and the interplanetary magnetic field increased in strength to 15 nT with a slight southward Bz (-5 to -10 nT). This transient activity resulted in a brief interval of geomagnetic storming (Kp=6-).

b. ACE Solar Wind Outages

The ACE RSTW/SWEPAM monitor, which measures the speed, temperature and density of solar wind particles passing the ACE satellite, experienced several outages due to high fluxes of energetic particles. Reliable real-time information on solar wind speed, density, and temperature, was unavailable when it was most needed by forecasters. RSTW data are commonly unavailable when the flux of greater than 30 MeV protons exceed approximately 50 PFU. SWEPAM data eventually returned to normal values when the solar particle events began to abate; however, this occurred after the geomagnetic storms were already in progress.

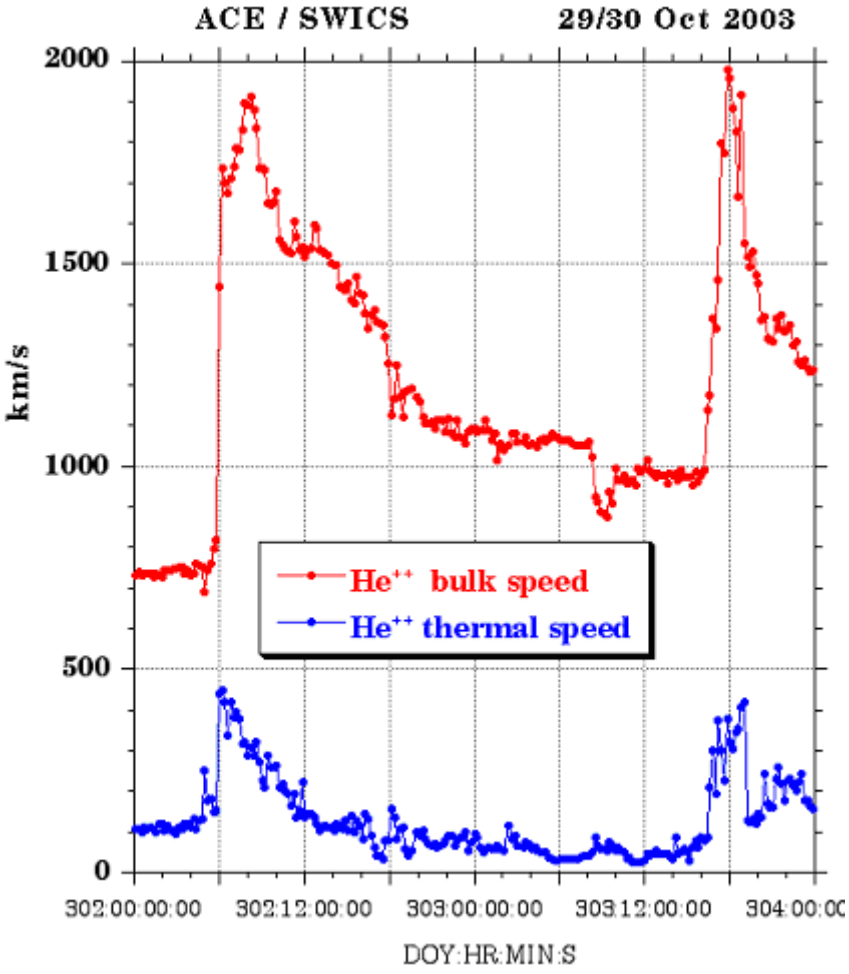

Figure 18: ACE SWICS estimated solar wind speed

The SWEPAM sensor was out of service beginning at 1220 UTC on 28 October, and recovered again at 0045 UTC on 31 October. Another outage was experienced at 1700 UTC on 2 November, and reliable service resumed after 2200 UTC.

Analysis of the scientific data from SWEPAM performed after the events provided a glimpse of the high-speed solar wind that passed Earth on early 29 October (Skoug, 2003). Estimates of the solar wind speed were made using SWEPAM "search mode," which collects data over a broad range of energies for 45 seconds every half hour, and is not subject to the same problems that occur with the real time sensor during high particle energies. The search mode data indicate solar wind speeds of about 2,000 km/s early on 29 October, at the time of transient flow driven by the X17 full-halo CME of 28 October. Figure 18 shows the estimated solar wind speed of helium as measured by the ACE/SWICS (Solar Wind Ion Composition Spectrometer) instrument. Subsequent analysis of SWICS data confirmed a maximum solar wind speed close to 2,000 km/s (Zurbuchen, et. al., 2004).

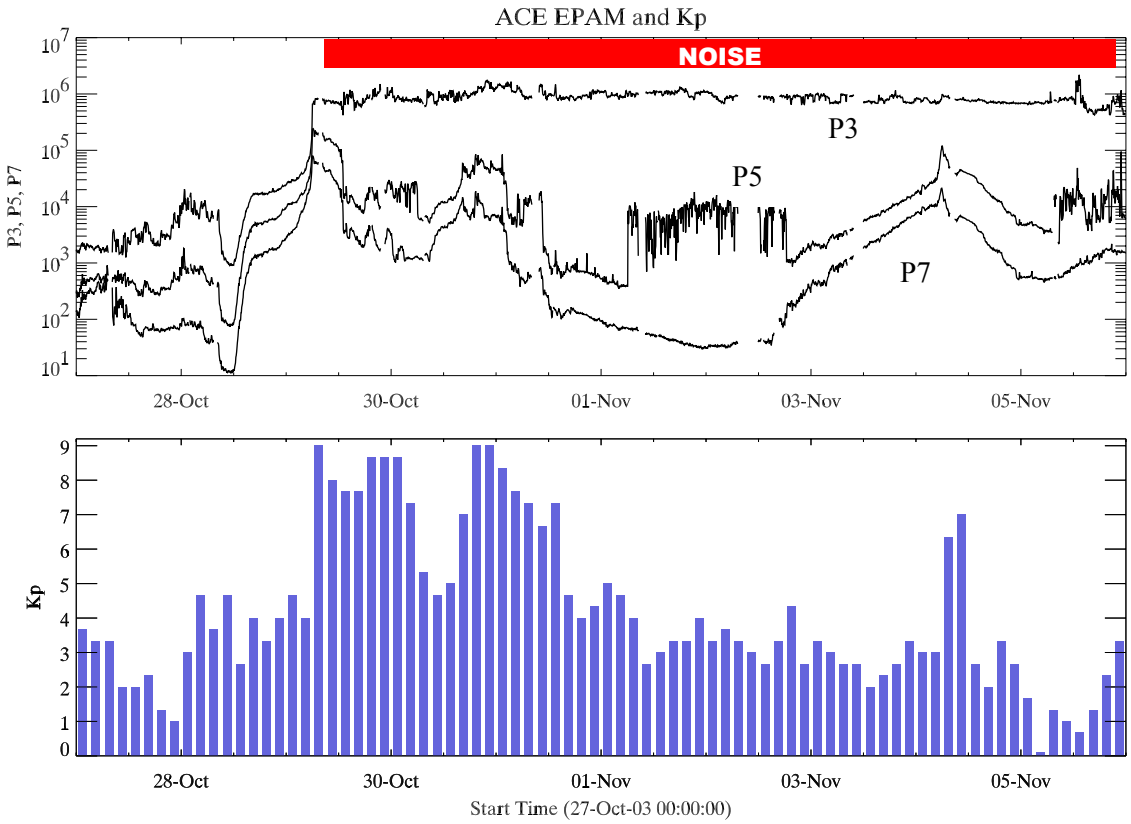

Figure 19: ACE EPAM and Kp from 28 October to 6 November 2003
(Noise can be seen on the P3 and P5 channels due to contamination from high energy particles)

c. ACE Energetic Particle Observations

Another unfortunate consequence of the intense solar radiation storms during the Halloween events was the impact on the ACE EPAM instrument. Along with the temporary loss of solar wind plasma data on SWEPAM, a more permanent problem developed with the ACE low energy ion measurements. Space weather forecasters use the ion flux monitored by EPAM to warn of an approaching interplanetary shock, which typically precedes a fast coronal mass ejection. The flux levels in the RTSW EPAM passbands are often seen to increase due to particles accelerated in front of the approaching shock front. This phenomena has become an important consideration for predicting the likelihood and onset of large geomagnetic storms. Indeed, the timing and intensity of the first severe geomagnetic storm in the Halloween events was correctly anticipated several hours prior to the storm onset due to the increase of the EPAM particles. Figure 19 illustrates the relationship between EPAM particle flux rise and subsequent geomagnetic storming, seen by the rise in the P3, P5, and P7 channels on 29 October at 0000 UTC up to the time of the shock arrival at 0559 UTC.

Unfortunately, the large energetic particle event raised the noise level of the P3 channel on the LEMS30 EPAM such that it was of very limited forecast value after the first CME arrived. Noise on the P3 and P5 channels can be seen in Figure 19. After several weeks, EPAM sensor

had not yet returned to normal operation and the loss of most of the data from this sensor may be permanent. The EPAM has another sensor (LEMS120) that produces similar data, and in February 2004 the data from LEMS120 replaced data from the damaged sensor and the RTSW system resumed normal operation.

4. GEOPHYSICAL EVENTS

a. Solar Proton Events

The interval of increased levels of space weather from 19 October to 7 November 2003 included four separate energetic proton events, including the fourth largest proton event at >10 MeV on record (Table 3). Two of these events were complex, consisting of multiple injections of energetic particles from separate sources, which led to multiple maxima within the events. These radiation storms were particularly noteworthy because of the widespread, significant effects they caused on a number of spacecraft (noted in Section 5).

Table 3: Top Radiation Storms Since 1976*

Rank	Peak Intensity (PFU)	Date
1	43,000	23/03/1991
2	40,000	19/10/1989
3	31,700	04/11/2001
4	**29,525**	**28/10/2003**
5	24,000	14/07/2000
6	18,900	22/11/2001
7	14,800	08/11/2000
8	12,900	24/09/2001
9	10,000	20/02/1994
10	9,200	12/08/1989
11	7,300	30/11/1989
12	4,600	09/05/1982
13	4,500	29/09/1989
14	3,500	08/03/1989
15	3,000	04/06/1991
16	2,900	11/06/1982
17	2,700	30/10/1992
18	2,520	21/04/2002
19	2,500	25/04/1984
20	2,360	01/10/2001

**Intesity measurements are from the GOES >10 MeV proton flux.*

The first event began at 1825 UTC on 26 October. Although there was some ambiguity about the solar origin of this event, the most likely candidate is the X1 flare from Region 484, which occurred near N02W38 on 26 October at 1819 UTC. The proton event maximum was 465 PFU at 2235 UTC. The event ended on 27 October at 0820 UTC. There was a small enhancement of the >100 MeV protons; however, the flux did not exceed the SEC alert threshold of 1 PFU.

The X17 flare from Region 486, which was centered near S16E08 on 28 October at 1110 UTC, produced both >10 MeV and >100 MeV proton events. The >10 MeV protons rose abruptly after the maximum of the flare, with the event beginning at 1215 UTC. The >10 MeV proton event maximum was 29,525 PFU at 0615 UTC on 29 October. This event is the fourth largest >10 MeV proton event on record. The X17 flare also produced a >100 MeV proton event, which began 5 minutes after the maximum of the flare, and reached event level at 1145 UTC on 28 October. This >100 MeV proton event reached a maximum of 186 PFU on 29 October at 0015 UTC (Figure 20).

There was a secondary >10 MeV proton enhancement that originated from an X10 flare from Region 486, which was centered at S15W02 on 29 October at 2049 UTC. There was already a >10 MeV event in progress at the time of this event. However, the onset of new particles from the X10 flare is clearly observed at about 2100 UTC. This enhancement produced a secondary maximum of 3298 PFU on 30 October at 1935 UTC. The greater than >10 MeV proton event finally dropped below threshold on 1 November at 1055 UTC. The X10 flare also produced a secondary enhancement in the >100 MeV protons. The enhancement produced a secondary maximum of 110 PFU on 29 October at 2310 UTC. The greater than >100 MeV proton event ended on 31 October at 0145 UTC.

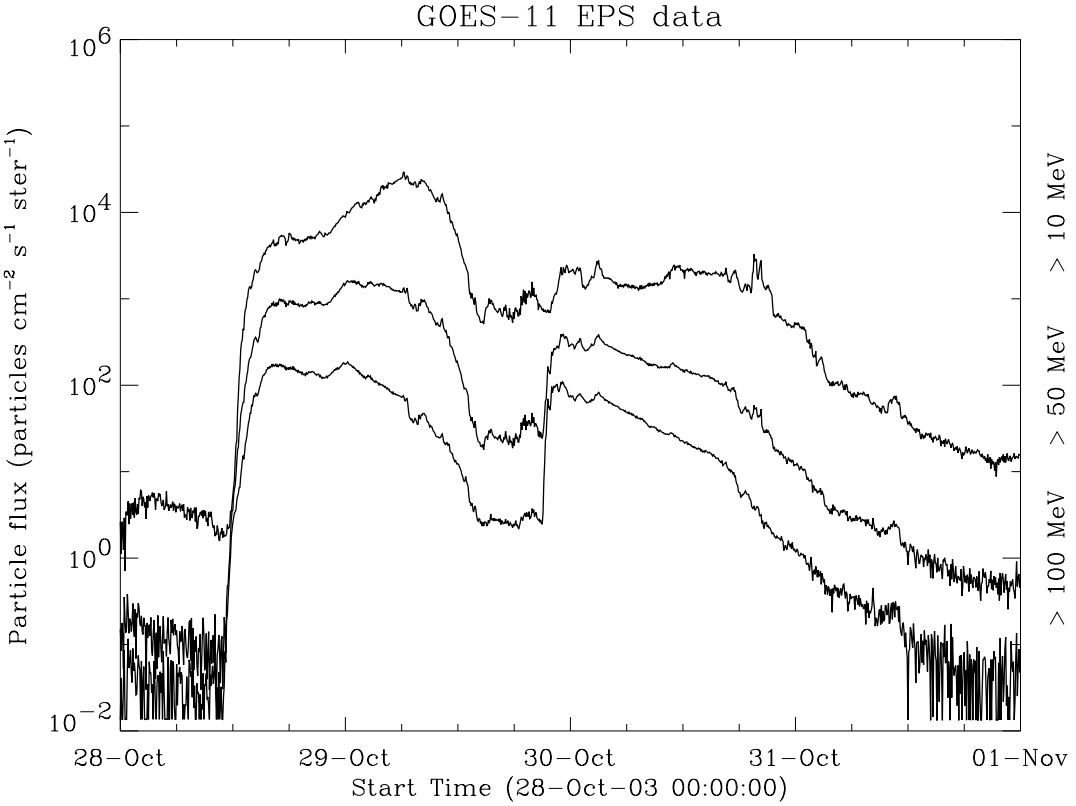

Figure 20: GOES Proton Flux, 28 through 31 October 2003

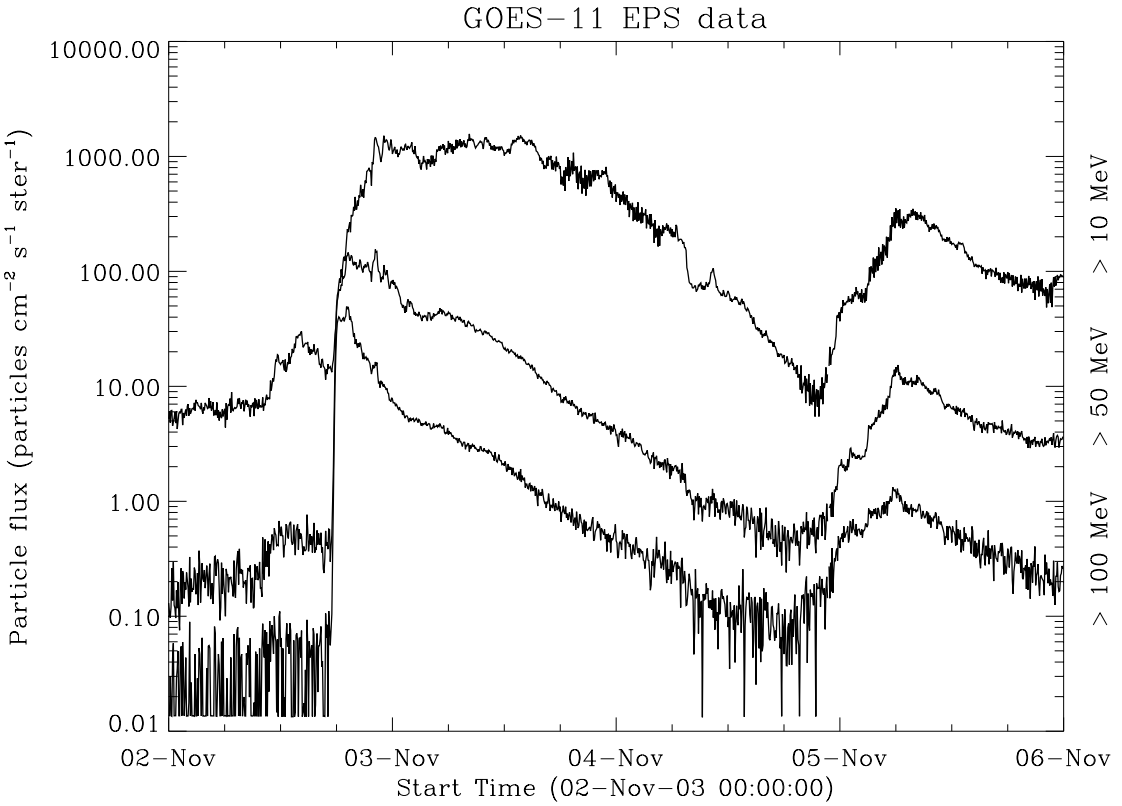

Figure 21: GOES Proton Flux, 2 through 5 November 2003

An M3 flare from Region 486 centered at S12W60 on 1 November at 2238 UTC produced a comparatively small >10 MeV proton event. The event began on 2 November at 1105 UTC and reached a maximum of 30 PFU on 2 November at 1415 UTC (Figure 20).

There was a secondary >10 MeV proton enhancement that was due to an X8 flare from Region 486 centered at S14W56 on 2 November at 1725 UTC. A >10 MeV proton event was already in progress when a rise was seen on the GOES-11 particle channels at about 1730 UTC. The rise was almost simultaneous with the maximum of the flare. This enhancement led to a secondary maximum of 1518 PFU on 3 November at 1345 UTC. The entire >10 MeV proton event then ended on 4 November at 2120 UTC. The X8 also produced a >100 MeV proton event. The event began on 2 November at 1740 UTC, reached a maximum of 49 PFU at 1905 UTC, and ended on 3 November at 1720 UTC (Figure 20).

The last >10 MeV proton event was from the X28 flare that occurred on 4 November at 1950 UTC from Region 486 centered at S19W83. The >10 MeV proton flux began to rise 2 hours 20 minutes after the maximum of the flare. The event threshold was crossed on 4 November at 2225 UTC and the event reached a maximum of 353 PFU on 5 November at 0600 UTC. This event then began a very gradual decline, finally ending on 7 November at 2115 UTC. The X28 produced a very gradual rise in the >100 MeV proton channel. The event took 3 hours 20 minutes from the time of flare maximum to begin to rise. The event threshold was crossed on 5 November at 0535 UTC, and maximum flux of 1 PFU was reached at 0540 UTC. The >100 MeV event ended at 0705 UTC.

Table 4: Top 30 geomagnetic storms based on Potsdam running Ap

Rank	Ap	Date
1	312	09/18/1941
2	293	11/12/1960
3	285	03/13/1989
4	277	03/24/1940
5	258	10/06/1960
6	**252**	**10/29/2003**
7	252	07/15/1959
8	251	03/31/1960
9	241	05/25/1967
10	229	07/13/1982
11	228	02/07/1986
12	226	03/29/1940
13	223	08/04/1972
14	222	07/05/1941
15	221	09/04/1957
16	**221**	**10/30/2003**
17	216	07/08/1958
18	215	03/28/1946
19	214	09/22/1946
20	212	03/01/1941
21	212	07/26/1946
22	203	08/19/1950
23	201	09/06/1982
24	199	02/07/1946
25	199	02/11/1958
26	196	05/12/1949
27	196	06/04/1991
28	195	03/24/1946
29	193	05/10/1992
30	192	07/15/2000

b. Geomagnetic Storms

There were five discrete, transient related geomagnetic storms during the period 19 October through 7 November. These included the sixth and sixteenth largest geomagnetic storms on record (since 1932), based on the Potsdam 24-hour running Ap index (Table 4). These two storms followed remarkably fast Sun to Earth CME transit times of under 20 hours.

24 – 25 October 2003

The storm onset on 24 October followed a 105 nT sudden impulse (SI) on the Boulder magnetometer at 1529 UTC. The likely source was the complex eruption and associated CME on 22 October from near Region 484. The storm began following an approximate 60-hour Sun to Earth transit of the CME. Though the storm was relatively weak, the sudden and intense change in dynamic pressure following the arrival of the interplanetary shock resulted in a considerable compression on

the magnetopause boundary. The Bz component of the interplanetary magnetic field went southward for a brief period following the SI, but quickly rotated into a prolonged strong northward orientation for the remainder of the transient flow. The highest Kp observed during the storm was a Kp=7-, observed at 1652 UTC on 24 October. The highest 24-hour running Ap for this storm was 43. The ~12-hour disturbance featured an initial brief severe storm period, followed by predominantly active to minor storm levels. The extended northward orientation of the IMF Bz likely thwarted a more significant geomagnetic response.

29 – 30 October 2003

The storm that began early on 29 October was the sixth largest geomagnetic storm on record based on the Potsdam running Ap index. The CME that drove this storm was associated with the powerful X17 flare from Region 486 on 28 October. The CME, traveling at over 2,200 km/s per second, made the Sun to Earth transit in remarkable time – less than 19 hours. A 140 nT sudden impulse was observed on the Boulder magnetometer on 29 October at 0613 UTC. Again, an intense compression of the magnetosphere occurred. The initial major storm conditions quickly elevated to severe levels, and the $Kp=9_0$ threshold was reached at 0839 UTC. Solar wind speeds near 1900 km/s and strong IMF variations in the sheath region of the interplanetary magnetic cloud, assured a significant response. The transition from the sheath into the plasma ejecta occurred within four hours of the shock arrival. IMF Bz went sharply northward and stayed that way for almost ten hours. However, geomagnetic storm levels stayed at or above the Kp=7 threshold for the duration of the northward Bz. This was largely due to the extreme nature of the solar wind speed buffeting the magnetosphere. IMF Bz rotated southward at around 1800 UTC on the 29th and the storm levels were again elevated in the Kp=8-9 range. The storm gradually weakened to minor storm levels early on 30 October. This intense geomagnetic storm, the largest of Solar Cycle 23, produced major to severe storm levels from onset at 0613 UTC on the 29 October through 0600 UTC on 30 October. The maximum running Ap was 252. The return to relative calm following the intense geomagnetic storm was short lived, as another fast and powerful CME loomed near.

30 – 31 October 2003

The geomagnetic field sustained primarily minor storm conditions from 0600-1600 UTC on 30 October as the storm of 29 October subsided. However, the X10 flare that occurred in Region 486 at 2049 UTC on 30 October produced another fast, Earth-directed halo CME. LASCO speed measurements suggested that this ejection was approximately 400 km/s slower than the 29 October event. However, following in the heels of the preceding CME, the ejecta propagated through very elevated solar wind speed, so deceleration of the CME through the interplanetary medium was minimal. The CME impacted Earth's magnetic field at around 1620 UTC on 30 October, after another remarkably fast ~19 hour Sun to Earth transit. Initial IMF Bz turning was strong southward and the geomagnetic response was intense. Planetary K values were in the 8-9 range with the most active periods occurring in the first six hours following storm commencement. By 0000 UTC on 1 November, the IMF Bz rotated northward; however, the extremely elevated solar wind speed sustained K values of 6 and 7 through midday on 31 October. The highest 24-hour running Ap for this storm was 220, making it the second strongest geomagnetic storm of Solar Cycle 23.

04 November 2003
The X8 flare from Region 486 on 02 November produced another powerful CME; however, most of the ejecta were directed off the southwest solar quadrant. A geomagnetic disturbance occurred, but the flanking passage of this CME limited the geomagnetic response. The shock impacted ACE at 0600 UTC on 04 November, approximately 37 hours after the eruption on the solar surface. A sudden impulse of 72 nT was observed by the Boulder magnetometer at 04/0627Z. The storm was short-lived with a maximum Kp of 7 and maximum Ap of 38. The topology of magnetic field and plasma measurements at ACE confirmed a flanking impact from this CME.

06 November 2003

The powerful X28 flare on 4 November produced an extremely fast CME off the southwest limb. While most of the ejecta did not appear to be Earth directed, a glancing blow was anticipated. A shock from the X28 flare reached Earth at 06/1937Z. A 31nT sudden impulse was observed on the Boulder magnetometer and activity briefly reached major storm levels. The maximum Kp was 6- and maximum Ap was 19.

c. Storm-time Disturbance Index (Dst)

There is another global index, Dst (storm-time disturbance), which was devised as a means of characterizing the level of disturbance observed in the equatorial regions (Suguira and Hendricks, 1967).[6] As has long been observed, the north-south horizontal component of the geomagnetic field becomes depressed during major geomagnetic storms and this is most pronounced in the low-latitude and equatorial regions. The degree and extent of this depression has proven to be a useful characterization of the energy transfer from the solar wind into the Earth's magnetosphere and is an estimate of the energy density of energetic particles in Earth's ring current.[7]

Table 5: Top 10 Dst Storms*

Rank	Dst (nT)	Date
1	-589	03/14/1989
2.	**-465****	**11/20/2003**
3.	-429	07/15/1959
4.	-427	09/13/1957
5.	-426	02/11/1958
6.	**-401****	**10/30/2003**
7.	-387	03/31/2001
8.	-387	05/26/1967
9.	-354	11/09/1991
10.	-339	11/13/1960

**Dst data from Kyoto World Data Center-C2 in Kyoto, Japan.*
***Provisional Dst – not the final value*

During the 29-30 geomagnetic storms, the preliminary Dst is estimated to have reached a maximum depression of -341 nT between 0100-0300 UTC on 30 October after which the index began to recover. However, after the onset of additional activity with the arrival of the second transient from the X10/CME, Dst started to show a second downward trend beginning at 1800 UTC and reached a second maximum of -401 nT between 2200-2300 UTC. It should be noted that Dst tends to behave like an integral of the geomagnetic drivers and that there is a time delay between the maximum of Dst depression and the peak of the high and subauroral latitude geomagnetic activity. For example, the highest levels of Kp were observed between 0600-0900 UTC on 29 October, almost 16 hours before the first maximum in Dst

[6] See also Mayaud 1980, and Campbell, 1997 for review material on the Dst index.
[7] Provisional measurements of the Dst index for the 29 and 30 October geomagnetic storms were made by the World Data Center-C2 in Kyoto Japan. See **http://swdcdb.kugi.kyoto-u.ac.jp/dstdir/** for more information.

occurred. During the second disturbance, peak Kp values were seen as early as the 1800-2100 UTC time window, which was at least an hour before Dst reached the secondary maximum. An examination of the historical record for geomagnetic storms as measured by Dst shows that the 29 October 2003 maximum of -401.0 is the 6th largest Dst storm on record (which dates back to 1957). Note also that if we treat the 30 October maximum of -341 nT as a separate storm from the 31 October maximum, then the 30 October storm would be the number 10 storm on the list (see Table 5).

d. Magnetopause Crossings

Earth's magnetopause is the boundary that separates the solar wind from the region in space dominated by Earth's magnetic field. On the line between Earth and the sun, the magnetopause is typically located about 10 Earth radii from Earth's center. On the downstream side, in the midnight region, the magnetopause forms the boundary of the elongated geomagnetic tail that extends for hundreds of Earth radii. When the solar wind dynamic pressure is very large and the interplanetary field is directed southward, conditions are ripe for moving the upstream, dayside magnetopause, from its typical location to a location closer to Earth and sometimes within geosynchronous orbit (6.6 Earth radii). At these times, when geosynchronous spacecraft on the dayside become located outside of Earth's magnetic field, they encounter highly variable magnetic fields that can be directed opposite to what is normally expected. These conditions can have undesirable effects on spacecraft that use torquer currents as part of their attitude control and momentum management. Under these conditions, spacecraft operators will sometimes turn off the spacecraft torquer currents to avoid torquing against the abnormal magnetic fields. Furthermore, the plasma environment surrounding the spacecraft is altered since the plasma density is often greater when the spacecraft crosses the magnetopause.

Table 6: Magnetopause Crossing Times

	GOES-8	**GOES-9**	**GOES-10**	**GOES-12**
24 October 2003			1832-1858	1525-1857
29 October 2003	2030-2400	0645-0650 1812-2400	1739-2327	1349-2057
30 October 2003	0000-0112 2006-2320	0000-0130 2035-2320	0004-0005 1736-2239	0033-0034 1737-2353

These estimated times (in UTC) are approximate and based on negative excursions of the Hp magnetic field component in the GOES 0.5 second sampled data. During some of these intervals, the magnetopause moved in an out over GOES many times.

During the Halloween Storms, the magnetopause crossed over the GOES satellites on numerous occasions. Table 6 gives the approximate times of these crossing intervals, which occur when GOES satellites are located on the dayside during the times of large solar wind pressure and large southward interplanetary magnetic fields.

The crossings observed on 29-31 October 2003 by the operational GOES 10 (bottom) and GOES 12 (top) satellites in 0.5 second sampled data are shown in Figure 22. GOES 10 and 12 are

located at 134.8 and 75.4 degrees west geographic longitude, respectively. The traces show the Hp component of the magnetic field measure by GOES which is the component parallel to Earth's spin axis. The typical dayside magnetic field in the Hp component is around 120 nT. A magnetopause crossing is clearly indicated when the dayside field switches sign and goes negative. That can be seen several times in the GOES 10 and 12 data during the interval in Figure 22. The label N on the figure indicate when the spacecraft are located at local noon.

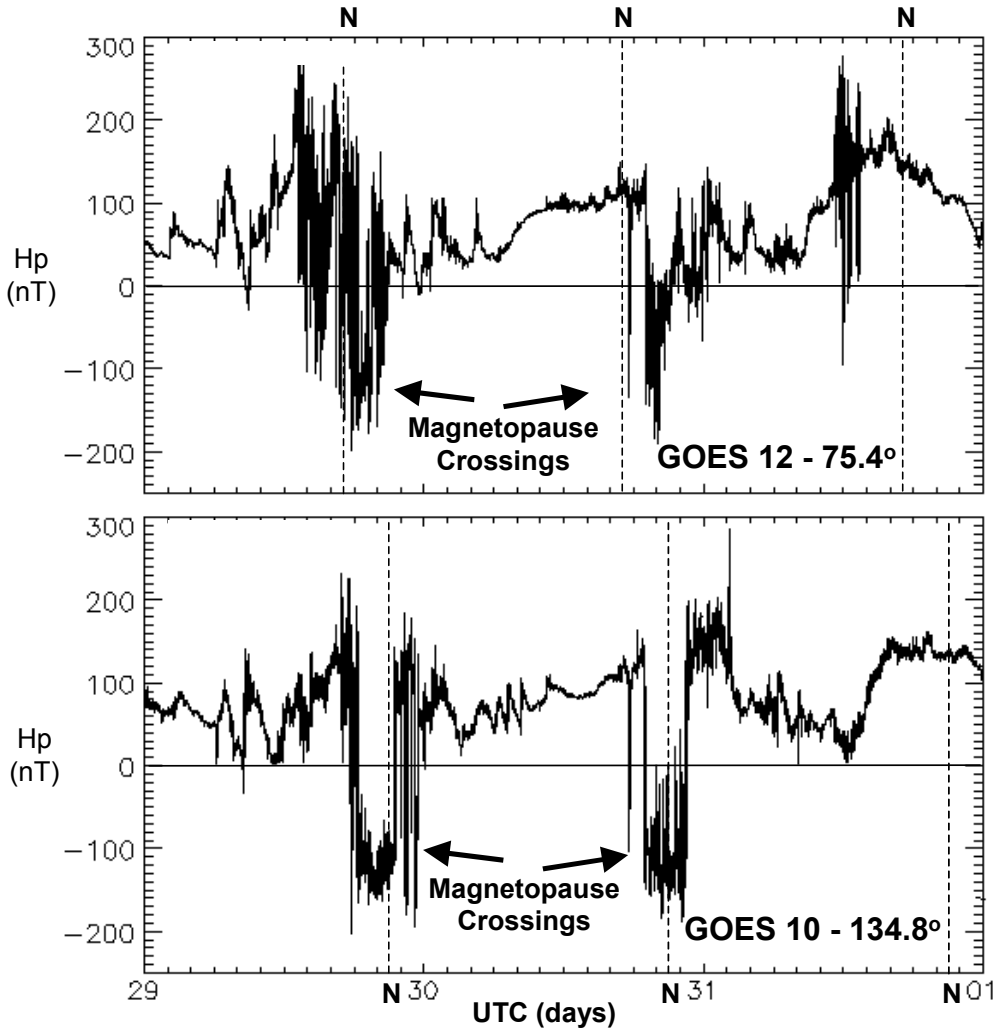

Figure 22: GOES Magnetopause Crossings on 29-31 October 2003.

e. Cosmic Rays (Ground Level Events and Forbush Decrease)

Neutron monitors around the world recorded activity on 28 and 29 October in the form of ground level events (GLE) and a Forbush decrease (FBD). Data from a number of neutron monitoring stations were collected and average values are presented in Table 7. The X17 flare on 28 October produced a ground level event with an average increase in neutron flux of 6% above background. The arrival of the CME related to the X17 flare produced a Forbush decrease in

neutron flux of 24% below background levels. The X10 flare on 29 October produced a GLE with an average increase in neutron flux of 9% above background. Although the ground level events were not above the 10% event threshold, enhancements were clearly observed on many neutron monitors. Antarctic stations at McMurdo and South Pole observed GLE and FBD levels much larger than the other stations. Values of a 17% GLE for the X17, 31% for the FBD, and a 24% GLE for the X10 flare were observed in Antarctica.

Table 7: Neutron Monitor Data

STATION	X17 GLE 28-Oct % Incr	FBD 29-Oct % Decr	X10 GLE 29-Oct % Incr
Thule	6	25	7
Oulu	9	27	9
Kiel	6	22	9
Kergue	6	26	11
Inuvik	7	26	8
Haleak	3	17	9
Climax	7	25	14
Cape S	5	25	9
Average	**6.1**	**24.1**	**9.5**
McMurdo	17	27	19
South Pole	16	35	28
Average	**16.5**	**31.0**	**23.5**

Data courtesy of the
World Data Center-C2 for Cosmic Rays
Ibaraki University, Mito, Japan

5. CUSTOMER SUPPORT AND IMPACTS

SEC's customer base is wide ranging and includes multiple agencies involved in deep space missions, satellite and space operations in near-Earth orbits, the airline industry, electric utilities, communications and navigation interests, and more. Support provided by SEC during the high solar activity period differed considerably from user to user. The following section will briefly address the impact of space weather on the various technologies both on Earth and in space and the support provided by SEC to assist these users.[8]

a. NASA Human Spaceflight and International Space Station

The NASA Space Radiation Analysis Group (SRAG) at the Johnson Space Center (JSC) is responsible for ensuring that the radiation exposure received by astronauts remains below established safety limits. Telephone briefings between SEC and SRAG are conducted daily, and the support tempo increases significantly during special operations such as space shuttle missions and extra-vehicular activity (space walks) and during periods of high solar activity. The extensive coordination between SEC and NASA resulted in actions by SRAG that ensured astronauts would not exceed acceptable risk from exposure to radiation, and cut the potential radiation exposure of the crew by approximately 50% by relocating the crew to a more sheltered section of the space station.

NASA also decided to do a ground-commanded power-down of the billion dollar ISS robotic arm and on-board workstation, which are more sensitive to higher than normal radiation events. They prepared to take other precautionary actions (e.g. shut down the S-band antenna controller and external color TV cameras) if radiation levels were to increase more than they did. The ISS Environments System Team also reported that the ISS experienced abnormal frictional drag.

b. NASA Deep-Space Missions

Numerous deep-space missions in progress during the October-November time frame were impacted by the severe solar activity. The lists of impacts below highlight some details of known anomalies.

Mars Odyssey – Spacecraft entered safe mode during the severe radiation storm. During downloading on 29 October, the spacecraft had a memory error that was corrected with a cold reboot on 31 October. The MARIE instrument on the Mars Odyssey had a temperature red alarm which required it to be powered off on 28 October. Recovery is not expected. Ironically, MARIE's mission was to assess the radiation environment at Mars in order to determine the radiation risk for astronauts on a Mars human spaceflight mission.

Stardust – Comet mission went into safe mode due to read errors. The mission has subsequently recovered.

[8] For more details on customer impacts and SEC support during the October-November Space Weather Storms see **Service Assessment: Intense Space Weather Storms October 19 – November 7, 2003**, March 2004.

SMART-1 – Spacecraft automatically shutdown the engine due to high radiation levels in lunar transfer orbit. SMART operators reported a total of 3 shutdowns.

Mars Explorer Rover – Spacecraft entered "Sun Idle" mode due to excessive star tracker error events. Operations were suspended during high solar activity and the system subsequently recovered.

Microwave Anisotropy Probe – The spacecraft star tracker reset, and the backup tracker autonomously turned on. The prime tracker has recovered.

Mars Express – The spacecraft had to use gyroscopes for stabilization, because the energetic particle event made it impossible to navigate using stars as reference points. The radiation storm blinded the orbiter's star trackers for 15 hours. The events also delayed a scheduled Beagle 2 checkout procedure.

c. Other Spacecraft

ADEOS-2 – Japan Aerospace Exploration Agency (JAXA) lost contact with the ADEOS-2 satellite, following an intense CME, which impacted Earth's magnetic field on 24 October. ADEOS-2 is an environmental observation satellite, launched in December 2002 by the Japanese Space Agency. It was designed to collect data on global warming and other climate-change phenomena. The spacecraft was developed at a cost of 70 billion yen ($640 million), and it had an expected lifespan of three years. Recovery is not expected.

Advanced Composition Explorer (ACE) – EPAM Low Energy Magnetic Spectrometer (LEMS 30) was damaged: Noise levels increased in several ion channels and remain abnormally elevated. Recovery is not expected.

SOHO – Both the Coronal Diagnostic Spectrometer (CDS) and the Ultraviolet Coronagraph Spectrometer (UVCS) were safed manually on 28 and 30 October, due to the elevated proton levels. Both instruments recovered. On November 4, the CDS/GIS instrument had 3 detectors trip autonomously, due to excessive count rates. The instrument was recovered later that same day.

Kodama, Data Relay Test Satellite (DRTS) – The spacecraft went into safe mode on the morning of October 29, during the severe (S4) solar radiation storm. The DRTS is a geostationary communications satellite that relays data among Low Earth Orbit (300-1,000 km altitude) spacecraft (including the International Space Station) and ground stations. Kodama was recovered on 7 November at 2119 JST.

CHIPS – The satellite computer went offline on 29 October and contact was lost with the spacecraft for 18 hours (loss of 3-axis control because its Single Board Computer (SBC) stopped executing). When contacted, the spacecraft was tumbling, but recovery was successful. It was offline for a total of 27 hrs.

DMSP F16 – The SSIES sensor lost data twice, on 28 October and 3 November. The sensor was recovered. The microwave sounder lost an oscillator. A switch to a redundant system was required to resume operation.

CHANDRA – Observations were halted on several occasions during the high solar activity, including an extended outage from 28 October to 1 November.

GOES-9, 10 and 12 – The spacecraft experienced high bit error rates (9 and 10) and magnetic torquers were disabled (12) due to solar activity.

Inmarsat (fleet of 9 geosynchronous satellites) – Controllers at its Satellite Control Centre had to quickly react to the solar activity to control Inmarsat's fleet of geosynchronous satellites. Two satellites experienced speed increases in momentum wheels which required firing of thrusters to mitigate. One satellite had an outage when its CPU went offline.

TV and Pay Radio Satellite Services: TV satellite controllers reported many problems with maintaining routine operations. They had to resort to "manual attitude control" for 18 hour to 24 hour periods due to magnetopause crossing events that affect the attitude controller of two or more of their fleet. A component has "burned out" in one circuit box in a newer satellite. The failure required a workaround which was successful. Pay radio satellite had several short-lived periods when they lost satellite signal lock.

Department of Defense: Satellite operations over high-interest regions were lost for 29 hours when three spacecraft either experienced anomalies or were shut down to avoid damage due to space weather.

d. Mitigating Actions Taken by Spacecraft Operations Teams

Aqua, Landsat, Terra, TOMS, TRMM – NASA's Earth Sciences Mission Office directed all instruments on these five spacecraft be turned off or safed due to a Level 5 storm prediction (29 October).

SIRTF – In orbit while drifting behind Earth, operators turned the science experiments off due to high proton fluxes (29 October). Four days of operations were lost.

The **CDS** instrument on **SOHO** spacecraft was placed into Safe mode for 3 days (28-30 October).

UARS/HALOE – The activation of the instrument was delayed due to activity.

Department of Defense – Air Force Space Command corrected for satellite orbit changes by running satellite drag models based on advanced warning of geomagnetic and solar activity indices.

e. Global Positioning System (GPS)

GPS operations are affected by changes in total electron content (TEC) of the ionosphere along the path to the satellite during large flares and geomagnetic storms. Significant storms can cause large increases and decreases in TEC, which impact the accuracy of single-frequency GPS. Dual-frequency GPS receivers can better adjust to a disturbed ionosphere, but still experience some degraded signals and position errors.

Many GPS users will experience little or no impact during TEC distrubances, but those requiring precise GPS measurements have a great need for SEC alerts and warnings. Those with the greatest concerns include surveying companies using GPS measurements for land surveying, topographic work, and property boundary analysis, deep-sea drilling operations, land drilling and mining, and various DoD operations.

Operators relying on GPS can and will take important actions during geomagnetic storms. During the October-November activity, companies delayed high resolution land surveying, postponed airborne and marine survey operations, cancelled drilling operations, and some, as was the case with the C.R. Luigs deep water drill ship, resorted to backup systems to ensure continuity of operations.

f. Airline Operations

The polar routes used by commercial airlines are impacted significantly by solar activity. Airlines on polar routes must contend with degraded communications; potential biological impacts from radiation storms; impacts to navigational systems (generally a lesser concern); and as avionics evolve, a potential impact to electronic systems. The October-November solar storms created a significant disruption to airline operations. Some polar flights were diverted, requiring additional stop-offs and resulting in additional fuel, flight time, and also costly crew exchanges.

HF/VHF Communications

Polar flights departing from North America use VHF (30-300 MHz) communication with Canadian Air Traffic Control (ATC) and Arctic Radio. When at high latitudes outside of the range of VHF, aircraft communicate via HF (3 – 30 MHz). Satellite Communications (SATCOM) is considered a backup during polar flights, but it is not available above 82 degrees North Latitude. Airlines and ground controllers experienced communications problems almost daily during the October – November solar activity outbreak. Initially (October 19 – 23), the degraded HF communications were due to elevated X-ray solar emissions and the moderate to strong solar flare activity. On October 19, following the X1 (R3) flare, Air Traffic Centers reported moderate-to-severe impacts on all HF groups and HF service was degraded for over two hours. In response, a major carrier rerouted three polar flights from Polar Route 3 to Polar Route 4 (Figure 7), which is more desirable for data-link and Satcom. This required an additional 26,600 pounds of fuel and resulted in over 16,500 pounds of cargo being denied. On 24 October 2003 following the onset of a G3 (strong) geomagnetic storm, Edmonton Air Traffic Control Center released a notice to airmen (NOTAM) and placed restrictions on airline operations in high-latitudes.

These were the first of several such periods of severely degraded communication. As each major flare occurred, HF communications at low and mid-latitudes underwent a range of problems from minor signal degradation to complete HF blackout. Higher latitudes experienced additional difficult periods following the onset of the radiation storms on 26 October.

Space Radiation Effects
Essentially all commercial aviation interests were made aware of the radiation storm levels on 28-29 October, when the Federal Aviation Administration (FAA) issued their first ever advisory suggesting that airline pilots stay below 25,000 feet when traveling above 35 degrees geomagnetic latitude, both north and south. This FAA product is based on the NOAA GOES particle sensors and is advisory only. Airlines are not required to take action based on this advisory. Several flights on the U.S. to Europe routes did fly at lower altitudes during this severe radiation storm. The FAA issued Solar Radiation Alerts on three occasions during the October-November activity.

Navigation
The FAA's Wide-Area Augmentations Systems (WAAS) was seriously impacted. For a 15-hour period on October 29 and an 11-hour interval on October 30, the ionosphere was so disturbed that the vertical error limit, as defined by the FAA's Lateral Navigation Vertical Navigation (LNAV/VNAV) specification to be no more than 50 meters, was exceeded. That translated into commercial aircraft being unable to use the WAAS for precision approaches.

g. Antarctic Operations

The Antarctic science groups and staff rely on a company called MacRelay to provide essential radio communications between McMurdo Station and remote sites on the Antarctic. MacRelay is also responsible for communication links with aircraft and ships supporting the United States Antarctic Program. The primary source of communication is HF radio. MacRelay experienced over 130 hours of HF communication blackout during the October – November activity.

Following an extended solar flare induced HF outage earlier in this solar cycle, McMurdo staff developed a contingency plan to use Iridium satellite phones as backup during HF outages. During the previous periods of severe solar activity, numerous support flights were delayed for several days, since take-off and landing restrictions are increased during HF blackouts. The LC-130 aircraft that service the remote sites use Iridium phones to communicate with McMurdo and the remote locations.

Scientific missions in the field (at camp) in Antarctica are required to 'check in' with MacRelay communications under normal circumstances via HF. If they miss their 'check in' then a rescue mission is considered. MacRelay was made aware that space weather was causing an HF blackout conditions, allowing them to implement contingency plans.

h. Electric Utilities

The geomagnetic storms on 29 and 30 October were certainly among the strongest this cycle. When a geomagnetic storm is in progress, the fluctuations of the geomagnetic field induce electric fields and this can drive potentially damaging geomagnetically induced currents (GIC) in electrical power lines and transformers. The late October storms caused GIC's that impacted power grids around the globe.

Power companies in North America experienced some problems during the October-November high solar activity. Impacts and actions reported by grid operators included less use and switching between systems, high levels of neutral current observed at stations throughout the country, a capacitor trip in the northwest (known to be GIC susceptible), and transformer heating in the Eastern U.S. Precautions were implemented. For example, a 'growling' transformer was backed down to help cool it. GIC impacts were more significant in Northern Europe where heating in a nuclear plant transformer was reported and a power system failure occurred on 30 October in Malmo, Sweden resulting in blackout conditions for about one hour.

Electrical companies took considerable efforts to prepare for and be aware of the storm onsets. Companies received the standard suite of geomagnetic storm watches, warnings and alerts, but SEC staff also supplemented standard support with several phone discussions. Preventive action helped to counter the GIC stresses that were observed. A representative from the North American Electric Reliability Council (NERC) commented: "Although the bulk electric system was not significantly affected by the solar activity, some systems reported higher than normal GIC's that resulted in fluctuations in the output of some generating units, while the output of other units was reduced in response to the K-index forecast." Responses to warnings included reducing system load, disconnecting system components, and postponing maintenance.

i. Aurora

The Aurora Borealis and Aurora Australis (northern and southern lights) are the visible manifestation of geomagnetic disturbances. With the advent of the Internet and other advances in communications, entrepreneurs are seizing commercial opportunities to provide aurora alerts, image galleries and photo sales, and even aurora viewing tours. The public's interest in aurora viewing generated numerous contacts from media and the general public.

Though it is not a part of SEC's product line, SEC staff assisted with numerous inquiries about aurora viewing. The extreme and prolonged geomagnetic storms on 29 and 30 October ensured widespread middle and even low latitude aurora. Aurora sightings occurred from California to Houston to Florida. Tremendous aurora viewing was also reported from mid-Europe and even as far south as the Mediterranean countries.

6. SUMMARY

The space weather storms of late October to early November 2003 constitute some of the highest levels of activity seen to date for solar cycle 23. This high activity interval began with the appearance of three large, complex sunspot Regions which we have discussed in detail in this document. Of these three, Region 486 developed into the largest sunspot group of the current solar cycle and became the dominant producer of spectacular solar events with significant geophysical consequences.

Among the 17 major flares that were observed during the period, the X17 on 28 October, the X10 on the 29 October, and the X28 on the 4 November and their associated coronal mass ejections stand out as extraordinary. The X17 on the 28 October is the 4th largest X-ray flare on record (which begins in 1976) and was followed by a rapid rise in the flux of energetic protons in the geospace environment. The proton flux continued to rise as a fast interplanetary shock transited from the Sun to Earth, in about 19 hours, leading to a peak flux of 29,525 PFU at >10 MeV with the arrival of the shock early on 29 October. Based on the peak >10 MeV flux, this is the 4th largest proton event observed since the records began in 1976. The arrival of the shock was followed by extreme levels of geomagnetic activity as measured by the planetary Kp/Ap indices and by the global Dst (provisional) index, with maximum Kp values of 9_0, a maximum running Ap value of 252, and a maximum Dst of –363 nT. Based on the running Ap-index, this is the 6th largest storm on record (which dates back to 1932) and based on the provisional Dst this is also the 6th largest storm on record (dating back to 1957).

The X10 flare and associated CME of 29 October were also remarkable for their subsequent geophysical effects. The event was followed by another rapid injection of energetic protons in the geospace environment, producing a secondary maximum up to 3298 PFU at >10 MeV, and prolonging the proton event through early on 31 October. The fast halo CME associated with this flare transited very rapidly from the Sun to Earth in about 19 hours and drove a new round of extreme geomagnetic activity, leading to additional Kp values of 9_0, a secondary maximum running Ap value of 220, and a secondary enhancement of the provisional Dst to –401 nT.

The X28 flare and fast CME on 4 November was an incredible finale for Region 486 as it transited the West limb. The X-ray flare is very likely the largest observed during the GOES/SMS observing era of the past 28 years and the CME speed of about 2,400 km/s is truly an extreme! Due to the location of 486 at the time of this event, however, the geophysical consequences at Earth were not as remarkable as the X17 and X10 events.

A wide range of effects on human activities and technological systems were observed. The most extensively reported effects were seen from the interaction of energetic particles with human spacecraft operations and spacecraft electronics. A number of specific deep space missions and near-earth satellites were affected, including a fatal anomaly on the MARIE instrument on the Mars Odyssey mission. The impact of this interval on airline operations is also particularly noteworthy. Airline routes and schedules were significantly affected because of communication degradation in the daylit and Polar Regions and because of concerns about increased radiation exposure at high latitudes.

Although the spacecraft and the airlines effects were most prevalent, it is also clear that a broader range of problems occurred, including HF/VHF communication systems, LF/VLF communications, Global Positioning System (GPS) applications, and electrical power systems. The disruption of electrical power in southern Sweden during the activity late on October 30th is certainly a significant example.

SEC prepared a **Service Assessment: Intense Space Weather Storms October 19 – November 7, 2003** to document in more detail the effects of the solar activity during this period, including findings and recommendations for SEC's forecast operations. This document is available on SEC's website.

What makes this interval of activity particularly noteworthy from a scientific and technical point of view is the diversity of space weather observations, which were being made, many of which were not available in the past during similar extreme space weather events. The high levels of geophysical impacts and the wide range of observations will undoubtedly lead to more detailed and extensive analyses of space weather than have been possible in the past. We have provided in this document the important context within which such analyses may be considered.

7. REFERENCES

Campbell, W. H., *Introduction to Geomagnetic Fields*, Cambridge University Press, New York, 1997.

Delaboudiniere, J-P, *Solar Physics* 162, 291, 1995.

Bruckner, G.E., *Solar Physics* 162, 357, 1995.

Mayaud, P. N., Derivation, Meaning, and Use of Geomagnetic Indices, *American Geophysical Union*, Washington, D. C., 1980.

NOAA SEC, *Service Assessment: Intense Space Weather Storms October 19 – November 7, 2003*, March 2004.

Skoug, R., personal communication, 2003.

Sugiura, M., and S. Hendricks, Provisional hourly values of the equatorial Dst for 1961, 1962, and 1963, *NASA Tech. Note D-4047*, 1967.

Webb, D. and J. Allen, Spacecraft and Ground Anomalies Related to the October-November 2003 Solar Activity, *Space Weather Quarterly*, Summer 2004.

Zurbuchen , T.H., G. Gloeckler, F. Ipavich, J. Raines, C.W. Smith, L.A. Fisk, On the fast coronal mass ejections in October/November 2003: ACE-SWICS results, unpublished manuscript, 2004.

Zwickl, R.D., K.A. Doggett, S. Sahm, W.P. Barrett, R.N. Grubb, T.R. Detman, V.J. Raben, The NOAA Real-Time Solar-Wind (RSTW) System Using ACE Date, *Space Science Reviews* 86: 633-648, 1998.

APPENDIX A: GLOSSARY OF TERMS AND ACRONYMS[9]

Ap – An index of the disturbance in the geomagnetic field, the planetary A index is calculated from a network of observations worldwide (for more information, see **http://www.gfz-potsdam.ge/pb2/pb23/Geomag/niemegk/kp-index**).

ACE – Advanced Composition Explorer is a research spacecraft built by NASA which measures particle energies over a wide range of energy and nuclear mass, and real-time solar wind data, from a vantage point approximately 1/100 of the distance from Earth to the Sun.

CME – Coronal Mass Ejection. A transient outflow of plasma through the solar corona into interplanetary space.

Coronograph – An optical device that enables observations of the white-light solar corona.

Dst – Storm-time Disturbance index. A measure of the variation in the geomagnetic field observed at low latitudes.

EIT – Extreme Ultraviolet Imaging Telescope. An instrument carried aboard the SOHO spacecraft that produces images of the Sun in several EUV wavelengths.

EPAM – Electron, Proton and Alpha Monitor. An instrument aboard the ACE spacecraft that measures the flux of energetic particles.

ESA – European Space Agency.

Full-halo CME – A CME that appears to expand completely around the solar disk. If a full-halo CME is associated with activity on the visible solar disk, then there is an increased possibility of interaction with Earth's magnetic field.

HF – High frequency.

Kp – A 3 hourly planetary index of geomagnetic activity calculated from a network of worldwide observations.

LASCO – Large Angle and Spectrometric Coronograph. A coronograph imager aboard the SOHO spacecraft.

LEMS – Low Energy Magnetic Spectrometers (on ACE)

MHz – Megahertz. Million cycles per second.

Millionth – A measure used to characterize the size of sunspot groups. 1 millionth of the size of the solar hemisphere visible from Earth.

NASA – National Aeronautics and Space Administration

nT – nanoTesla. A measure of magnetic field intensity.

PCA – Polar Cap Absorption. An anomalous condition of the polar ionosphere whereby HF and VHF radiowaves are absorbed, and LF and VLF radiowaves are reflected at lower altitudes than normal.

PFU – Particle flux unit = 1 particle cm^{-2} s^{-1} sr^{-1}.

[9] Further explanation of these terms can be found on SEC's online Glossary of Solar-Terrestrial Terms at **http://www.sec.noaa.gov/info/glossary.html**.

Radio Burst – An enhancement of radio emission from the Sun often associated with solar flare activity.

RTSW – Real Time Solar Wind. Refers to a subset of ACE data transmitted in real time.

SEC – Space Environment Center

SFU – Solar flux unit = 10^{-22} W m^{-2} Hz^{-1}

SI – Sudden Impulse. A sudden perturbation, positive or negative, of several nanoTeslas in the northward component of the low- and mid-latitude geomagnetic field.

SOHO – Solar and Heliospheric Observatory. A spacecraft launched by the European Space Agency (ESA) and NASA to study the Sun.

SSN – Smoothed Sunspot Number

SWEPAM – Solar Wind Electron, Proton, and Alpha Monitor. An instrument aboard the ACE spacecraft that provides observations of solar wind plasma parameters (density, velocity, and temperature).

SWICS – Solar Wind Ion Composition Spectrometer**.** An instrument aboard the ACE spacecraft that provides observations of the solar wind.

Tenflare – A solar flare accompanied by a 10-cm radio noise burst of intensity greater than 100% of the background level.

Type II Radio Sweep Narrow-band emission that begins in the meter range (300 MHz) and sweeps slowly (tens of minutes) toward deka-meter wavelengths (10 MHz). Type II emissions occur in loose association with major flares and are indicative of a shock wave moving through the solar atmosphere.

Type IV Radio Sweep – A smooth continuum of broad-band bursts primarily in the meter range (300 - 30 MHz). These bursts are generally associated with major flares beginning 10 to 20 minutes after the flare maximum, and can last for hours.

XRS – X-ray Sensor aboard the GOES spacecraft that measures X-ray flux.

APPENDIX B: SEC SPACE WEATHER ADVISORIES

SPACE WEATHER ADVISORY BULLETIN #03- 2
2003 October 21 at 06:11 p.m. MDT (2003 October 22 0011 UTC)

******* INTENSE ACTIVE REGIONS EMERGE ON SUN *******

Two very dynamic centers of activity have emerged on the Sun. NOAA Region 484 developed rapidly over the past three days and is now one of the largest sunspot clusters to emerge during Solar Cycle 23, approximately 10 times larger than Earth. This region, which is nearing the center of the solar disk, already produced a major flare (category R3 Radio Blackout on the NOAA Space Weather Scales) on 19 October at 1650 UTC. The region continues to grow, and additional substantial flare activity is likely.

A second intense active region is rotating around the southeast limb of the Sun. Though the sunspot group is not yet visible, two powerful eruptions occurred on 21 October as seen from the LASCO instrument on the SOHO spacecraft. These eruptions may herald the arrival of a volatile active center with the potential to impact various Earth systems.

Further major eruptions are possible from these active regions as they rotate across the face of the Sun over the next two weeks. Agencies impacted by solar flare radio blackouts, geomagnetic storms, and solar radiation storms may experience disruptions over this two-week period. These include satellite and other spacecraft operations, power systems, HF communications, and navigation systems.

SPACE WEATHER ADVISORY BULLETIN #03- 3
2003 October 28 at 10:55 a.m. MST (2003 October 28 1755 UTC)

******* SOLAR ACTIVE REGION PRODUCES INTENSE SOLAR FLARE *******

The dynamic solar regions reported on 21 October continue to produce high levels of solar activity. NOAA Region 486 produced a category R4 (severe) radio blackout with an associated category S3 (strong) solar radiation storm on 28 October at 1110 UTC (6:10 A.M. EST). The SOHO/LASCO instruments also observed a full halo coronal mass ejection with this activity, which is Earth directed. This region is the second largest in size this solar cycle.

As a result of this activity a category G4 (severe) geomagnetic storm is expected with periods of category G5 (extreme) levels possible. The solar radiation storm is also expected to continue at strong (G3) levels for the next 48 hours. Further major eruptions are possible from these active regions as they rotate across the face of the Sun over the next few days.

APPENDIX C: SPACE WEATHER SCALE OBSERVATIONS

	October													November						
	19	20	21	22	23	24	25	26	27	28	29	30	31	1	2	3	4	5	6	7
Radio Blackouts	R3	R1	R2	R2	R3	R2	R1	R3	R2	R4	R4	R1	R1	R1	R3	R3	R5	R2		
Geomag Storms	G1	G2	G2	G1		G3				G1	G5	G5	G4	G1			G3		G2	
Radiation Storms								S2	S2	S3	S4	S3	S2	S1	S2	S3	S2	S2	S1	S1

APPENDIX D: ENERGETIC EVENT SUMMARY

Energetic Events (M5 or greater)

Date	Time			X-ray		Optical Information			Peak Radio Flux		Sweep Freq Intensity	
	Begin	Max	½ Max	Class	Integ Flux	Imp/ Brtns	Location Lat	CMD	Rgn #	245	2695	II	IV
22 Oct	1947	2007	2028	M9.9	.160	Sf	S18E78		486	100	240		
23 Oct	0819	0835	0849	X5.4	.600	1b	S21E88		486	10000	1500	3	
23 Oct	1950	2004	2014	X1.1	.098	1n	S17E84		486	2500	77		
24 Oct	0227	0254	0314	M7.6	.160	1n	S19E72		486	6800	73	2	
26 Oct	0557	0654	0733	X1.2	.510	3b	S15E44		486	14000	4000	3	3
26 Oct	1721	1819	1921	X1.2	.630	1n	N02W38		484	1100	2000	2	
26 Oct	2134	2140	2148	M7.6	.043	2n	N01W38		484	57			
27 Oct	0921	0927	0932	M5.	.026	Sf	S16E26		486	65			
27 Oct	1227	1243	1252	M6.7	.064	Sf	S17E25		486	420	59		
28 Oct	0951	1110	1124	X17.	1.800	4b	S16E08		486	490000	13000	3	3
29 Oct	2037	2049	2101	X10.	.870	2b	S15W02		486	360000	2500	3	2
02 Nov	1703	1725	1739	X8.3	.910	2b	S14W56		486	24000	7700	3	3
03 Nov	0109	0130	0145	X2.7	.360	2b	N10W83		488	100	240	1	3
03 Nov	0943	0955	1019	X3.9	.560	2f	N08W77		488	3900	4400	2	1
04 Nov	1929	1950	2006	X28 .	2.300	3b	S19W83		486	4800	20000	3	2
05 Nov	1046	1052	1056	M5.3	.017	Sf	S16W90		486				

APPENDIX E: SOLAR ACTIVE REGION SUMMARIES

Region 484 Summary

Location			Sunspot Characteristics					Flares							
								X-ray			Optical				
Date	(° Lat ° CMD)	Helio Lon	Area (10^{-6} hemi)	Extent (helio)	Spot Class	Spot Count	Mag Class	C	M	X	S	1	2	3	4
18 Oct	N05E68	351	0240	04	Dac	020	B	9			8	2			
19 Oct	N06E53	353	1030	10	Dkc	028	Bgd	2	2	1	9	2			
20 Oct	N05E40	353	1420	11	Ekc	046	Bgd	7	1		7	1			
21 Oct	N04E26	354	1720	16	Dkc	069	Bgd	3	1		7				
22 Oct	N04E13	354	1750	11	Ekc	056	Bgd		2		16				
23 Oct	N04W00	354	1750	13	Ekc	053	Bgd		3		6	1			
24 Oct	N05W15	355	1460	12	Ekc	067	Bgd	2	1		6	1			
25 Oct	N04W28	355	1700	10	Dkc	052	Bgd	2	2		5				
26 Oct	N03W41	355	1350	11	Ekc	057	Bgd		2	1	1	1	1		
27 Oct	N03W54	355	1440	10	Dkc	029	Bgd	1	2		7	1	1		
28 Oct	N03W68	355	1240	09	Dkc	015	Bgd	2			1	3	1		
29 Oct	N03W82	356	0530	11	Eki	014	Bg								
30 Oct	N01W95	356	0210	10	Dao	006	Bg								
								28	16	2	73	12	3	0	0

Region 486 Summary

Location			Sunspot Characteristics					Flares							
								X-ray			Optical				
Date	(° Lat ° CMD)	Helio Lon	Area (10^{-6} hemi)	Extent (helio)	Spot Class	Spot Count	Mag Class	C	M	X	S	1	2	3	4
22 Oct	S16E81	286	0150	05	Hkx	001	A		4		1				
23 Oct	S16E70	285	1160	14	Ekc	024	Bgd			2		2			
24 Oct	S16E57	283	1540	16	Fkc	049	Bgd	1	2		3	2			
25 Oct	S15E45	282	2200	18	Fkc	052	Bgd		1		3		1		
26 Oct	S15E31	283	2170	19	Fkc	094	Bgd			1	2			1	
27 Oct	S16E18	283	2180	19	Fkc	074	Bgd	4	2		7				
28 Oct	S17E04	283	2120	19	Fkc	055	Bgd	1		1	9				1
29 Oct	S16W11	285	2610	18	Fkc	108	Bgd	2	2	1	4	2	1		
30 Oct	S18W23	284	2600	18	Fkc	080	Bgd		1		1				
31 Oct	S17W36	284	2030	20	Fkc	069	Bgd	1			3				
01 Nov	S17W49	284	1900	16	Fkc	099	Bgd	4	1		5	1			
02 Nov	S17W62	284	2160	16	Fkc	060	Bgd	1	1	1	5		1		
03 Nov	S17W75	284	1430	15	Fkc	016	Bgd		1		5				
04 Nov	S17W89	284	0630	13	Ekc	015	Bgd	2	1	1	1			1	
								16	16	7	49	7	3	2	1

Region 488 Summary

	Location		Sunspot Characteristics					Flares							
								X-ray			Optical				
Date	(° Lat ° CMD)	Helio Lon	Area (10^{-6} hemi)	Extent (helio)	Spot Class	Spot Count	Mag Class	C	M	X	S	1	2	3	4
27 Oct	N09E09	292	0270	08	Dko	020	B	3	1		9				
28 Oct	N08W04	291	0800	10	Dkc	034	Bgd	2			16	1			
29 Oct	N07W17	291	1460	16	Fkc	061	Bgd	1			6				
30 Oct	N08W28	289	1750	17	Fkc	034	Bgd	3	1			1			
31 Oct	N08W42	290	1570	17	Fkc	045	Bgd	4	1		8				
01 Nov	N08W55	290	1610	17	Fkc	040	Bgd	4	2		5				
02 Nov	N08W68	290	1600	16	Fkc	023	Bgd		1	2	3				
03 Nov	N08W82	290	1250	19	Fkc	009	Bgd			2	1		2		
04 Nov	N08W95	290	0320	08	Hax	001	A		1						
								17	7	3	48	2	2	0	0